# Bridging onshore and offshore present-day kinematics of central and eastern Méditerranean: Implications for crustal dynamics and mantle flow

Eugénie Pérouse, Nicolas Chamot-Rooke, Alain Rabaute, Pierre Briole, François Jouanne, Ivan Georgiev, Dimitar Dimitrov

Geochemistry Geophysics Geosystems G3

Article
Volume 13, Number 9
26 September 2012
Q09013, doi:10.1029/2012GC004289
ISSN: 1525-2027

Published by AGU and the Geochemical Society

# Bridging onshore and offshore present-day kinematics of central and eastern Mediterranean: Implications for crustal dynamics and mantle flow

**Eugénie Pérouse and Nicolas Chamot-Rooke**
*Laboratoire de Géologie, UMR CNRS 8538, Ecole Normale Supérieure, 24 Rue Lhomond, FR-75005 Paris, France (perouse@geologie.ens.fr)*

**Alain Rabaute**
*Laboratoire de Géologie, UMR CNRS 8538, Ecole Normale Supérieure, 24 Rue Lhomond, FR-75005 Paris, France*

*Now at Institut des Sciences de la Terre de Paris, UMR CNRS 7193, Université Paris VI Pierre et Marie Curie, FR-75252 Paris CEDEX 05, France*

**Pierre Briole**
*Laboratoire de Géologie, UMR CNRS 8538, Ecole Normale Supérieure, 24 Rue Lhomond, FR-75005 Paris, France*

**François Jouanne**
*Institut des Sciences de la Terre, UMR CNRS 5275, Université de Savoie, Campus Scientifique, FR-73370 Le Bourget-du-Lac, France*

**Ivan Georgiev and Dimitar Dimitrov**
*Department of Geodesy, National Institute of Geophysics, Geodesy and Geography, Bulgarian Academy of Sciences, Acad. G. Bonchev str, bl. 3, 1113 Sofia, Bulgaria*

[1] We present a new kinematic and strain model of an area encompassing the Calabrian and Hellenic subduction zones, western Anatolia and the Balkans. Using Haines and Holt's (1993) method, we derive continuous velocity and strain rate fields by interpolating geodetic velocities, including recent GPS data in the Balkans. Relative motion between stable Eurasia and the western Aegean Sea is gradually accommodated by distributed N-S extension from Southern Balkans to the Eastern Corinth Gulf, so that the westward propagation of the North Anatolian Fault (NAF) throughout continental Greece or Peloponnesus is not required. We thus propose that the NAF terminates in north Aegean and that N-S extension localized in the Corinth Gulf and distributed in Southern Balkans is due to the retreat of the Hellenic slab. The motion of the Hyblean plateau, Apulia Peninsula, south Adriatic Sea, Ionian Basin and Sirte plain can be minimized by a single rigid rotation around a pole located in the Sirte plain, compatible with the opening the Pelagian rifts (2–2.5 mm/yr) and seismotectonics in Libya. We interpret the trenchward ultraslow motion of the Calabrian arc (2–2.5 mm/yr) as pure collapse, the Calabrian subduction being now inactive. In the absolute plate motion reference frame, our modeled velocity field depicts two toroïdal crustal patterns located at both ends of the Hellenic subduction zone, clockwise in NW Greece and counter-clockwise in western Anatolia. We suggest the NW Greece toroïdal pattern is the surface expression of a slab tear and consequent toroïdal asthenospheric flow.

**Components:** 13,700 words, 13 figures, 2 tables.

**Keywords:** Balkans; Mediterranean; North Anatolian Fault; current plate motion; strain modeling; toroïdal flow.

**Index Terms:** 8120 Tectonophysics: Dynamics of lithosphere and mantle: general (1213); 8150 Tectonophysics: Plate boundary: general (3040); 8158 Tectonophysics: Plate motions: present and recent (3040).

**Received** 13 June 2012; **Revised** 20 August 2012; **Accepted** 21 August 2012; **Published** 26 September 2012.

Pérouse, E., N. Chamot-Rooke, A. Rabaute, P. Briole, F. Jouanne, I. Georgiev, and D. Dimitrov (2012), Bridging onshore and offshore present-day kinematics of central and eastern Mediterranean: Implications for crustal dynamics and mantle flow, *Geochem. Geophys. Geosyst.*, *13*, Q09013, doi:10.1029/2012GC004289.

## 1. Introduction

[2] The Mediterranean realm is one of these few natural laboratories where geodynamic processes can be studied through their interactions. Progressive closure of the space between the converging African and Eurasian plates has ultimately led to the present-day complex tectonic pattern, evolving – west to east – from tectonic inversion along the Maghrebian margin to ultraslow Calabrian subduction in the Central Mediterranean and to rapid subduction in the Hellenic trenches (Figure 1). Although the rates of motion are now well established following decades of geodetic measurements, the relative importance of the forces that drive the upper plate and lower plate deformation is still a matter of discussion.

[3] In the Central Mediterranean, the present-day motions are interpreted as micro-blocks interaction resulting from the fragmentation of the Apulian promontory [*Serpelloni et al.*, 2005; *D'Agostino et al.*, 2008]. Limits of these blocks remain unclear since a sizable portion of the Central Mediterranean is offshore (Ionian Basin, Adriatic Sea, Figure 1). In the Eastern Mediterranean, the kinematic pattern has been interpreted diversely as: a mosaic of rigid micro-blocks with deformation restricted to their boundaries [*Taymaz et al.*, 1991; *Goldsworthy et al.*, 2002; *Nyst and Thatcher*, 2004; *Reilinger et al.*, 2006; *Shaw and Jackson*, 2010]; large rigid domains combined with distributed deformation areas [*Le Pichon et al.*, 1995; *McClusky et al.*, 2000; *Le Pichon and Kreemer*, 2010; *Reilinger et al.*, 2010]; westward extrusion of Anatolia combined with widespread Aegean back-arc extension [*Armijo et al.*, 1996; *Flerit et al.*, 2004]; distributed deformation [*Papazachos*, 2002; *Floyd et al.*, 2010]. Whether active tectonics in the Aegean is caused by the westward propagation of the North Anatolian Fault [*Armijo et al.*, 1996; *Goldsworthy et al.*, 2002; *Flerit et al.*, 2004; *Shaw and Jackson*, 2010] or by basal shear and gravitational collapse associated to the retreat of the Hellenic slab [*Jolivet*, 2001; *Le Pourhiet et al.*, 2003; *Jolivet et al.*, 2008; *Jolivet et al.*, 2010] is still debated.

[4] Previous kinematic and geodynamic works have focused either on Central or Eastern Mediterranean, and little effort has been made to produce a self-consistent kinematic solution that simultaneously fits Calabria and Hellenic geodetic data as well as onshore and offshore constraints. Deformation in the Balkans [*Burchfiel et al.*, 2006; *Kotzev et al.*, 2006], emphasized by recent GPS studies [*Jouanne et al.*, 2012; K. Matev et al., Horizontal movements and strain rates obtained from GPS observations for the period 1996–2008 in southwest Bulgaria and northern Greece, manuscript in preparation, 2012] (Figure 2), has not always been considered, while fragmentation of the Nubian plate [*D'Agostino et al.*, 2008] is generally neglected.

[5] In this paper, we propose a large-scale kinematic model considering both subduction zones affecting and consuming the Nubian plate (Calabrian and Hellenic), as well as deformation of the Nubian plate itself (Ionian block) and of the entire Aegean-Anatolian-Balkans domain. *Haines and Holt* [1993]'s method is used to derive a continuous velocity and strain rate field by interpolating published GPS velocities, with particular attention to the offshore kinematics in the Ionian Basin and Adriatic Sea, that are key areas to bridge the gap between Central and Eastern Mediterranean. Our results are discussed in the light of: (1) the kinematic and possible dynamic interaction between the Southern Balkans, the Aegean and the supposed westward propagation of the NAF; (2) kinematics and boundaries of micro-blocks in the Central Mediterranean; (3) relationship

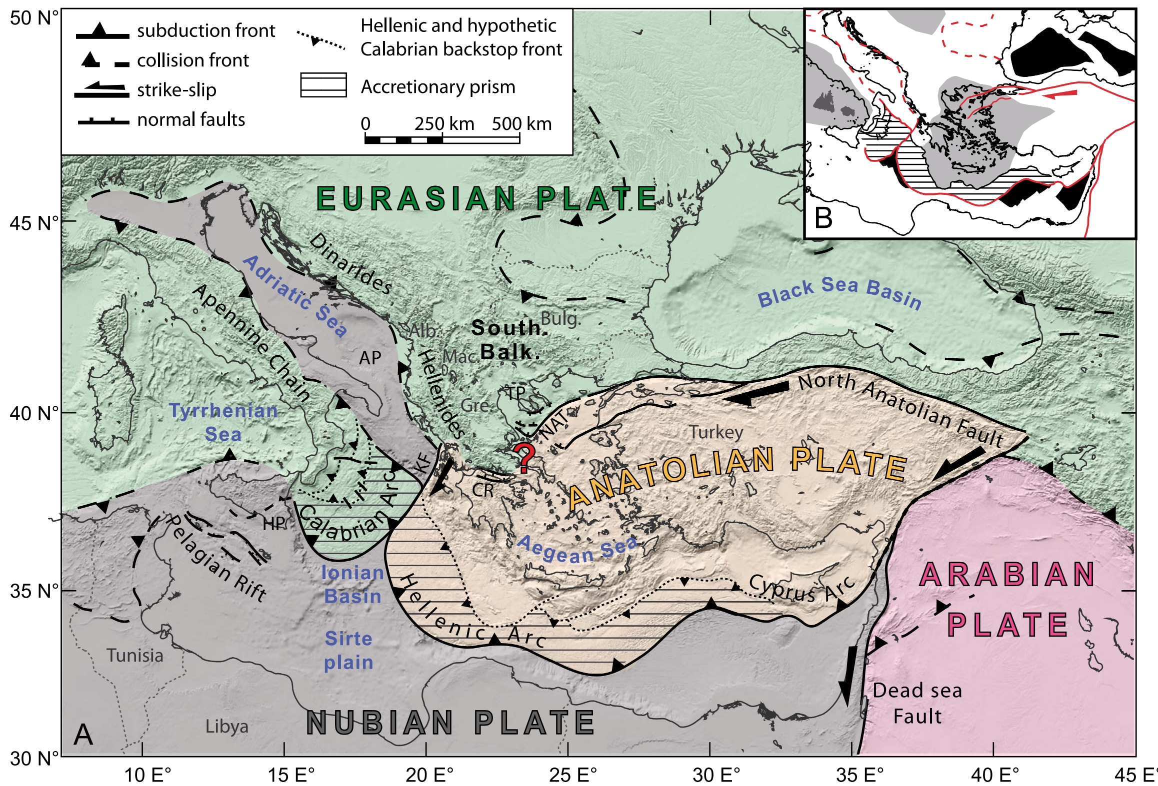


**Figure 1.** (a) Tectonic map of the Central and Eastern Mediterranean region with simplified plates model, modified from *Chamot-Rooke et al.* [2005]. South. Balk.: Southern Balkans; Alb.: Albania; Mac.: Macedonia; Bulg.: Bulgaria; Gre.: Greece; AP: Apulian platform; HP: Hyblean Plateau; KF: Kefalonia Fault; CR: Corinth Rift; TP: Thessaloniki Peninsula; NAT: North Aegean Trough. (b) Inset showing the nature of the crust in the region [*Chamot-Rooke et al.*, 2005; *Jolivet et al.*, 2008]. Black: Mesozoic remnant oceanic crust; dark gray: Neogene oceanic crust; light gray: Miocene post-orogenic thinned continental crust; white: continental crust; dashed line: accretionary prism over the crust.

between crustal dynamics and subduction induced mantle flows and slab tears.

## 2. Tectonic Settings

[6] Geological evolution of the Central and Eastern Mediterranean has been largely controlled by the build up and collapse of the Alpine orogenic belt during Cenozoic times, coeval with Mesozoic to present-day Africa-Arabia convergence toward Eurasia. Closure of the Tethyan basins and subsequent collision of the Apulian continent against Eurasia led to the Alpine belt orogeny in Late Cretaceous - Late Eocene (Apennines and Rhodope-Hellenides belts in Western and Eastern Mediterranean respectively [e.g., *Dewey et al.*, 1989]). The Apulian continent has been separated from the African margin by the opening of the Ionian Sea (westernmost branch of the Neo-Tethys [*Stampfli and Borel*, 2002]) that would have ceased in Early Jurassic [*Rosenbaum et al.*, 2004]. From that time, Africa and Apulian continents remained attached and moved together [*Channell*, 1996; *Rosenbaum et al.*, 2004]. Collapse of the Alpine belt in the Mediterranean region occurred in Miocene times. A drastic change in boundary conditions around Late Miocene – Pliocene times affected both the Central and Eastern Mediterranean. We briefly describe below the Miocene to present-day geodynamics.

### 2.1. Eastern Mediterranean

[7] Gravitational collapse of thickened crust associated with southward retreat of the Hellenic slab, consuming the remnant Mesozoic Ionian Sea oceanic crust toward the south, and back arc extension in the Aegean Sea took place from Early Miocene to Late Miocene [*Gautier et al.*, 1999; *Brun and Faccenna*, 2008; *Jolivet et al.*, 2008; *Jolivet and Brun*, 2010]. In addition to low-angle detachment faults in the Aegean Sea, western Anatolia [e.g., *Jolivet and Brun*, 2010], northern Greece and SW Bulgaria [e.g., *Burchfiel et al.*, 2008; *Brun and

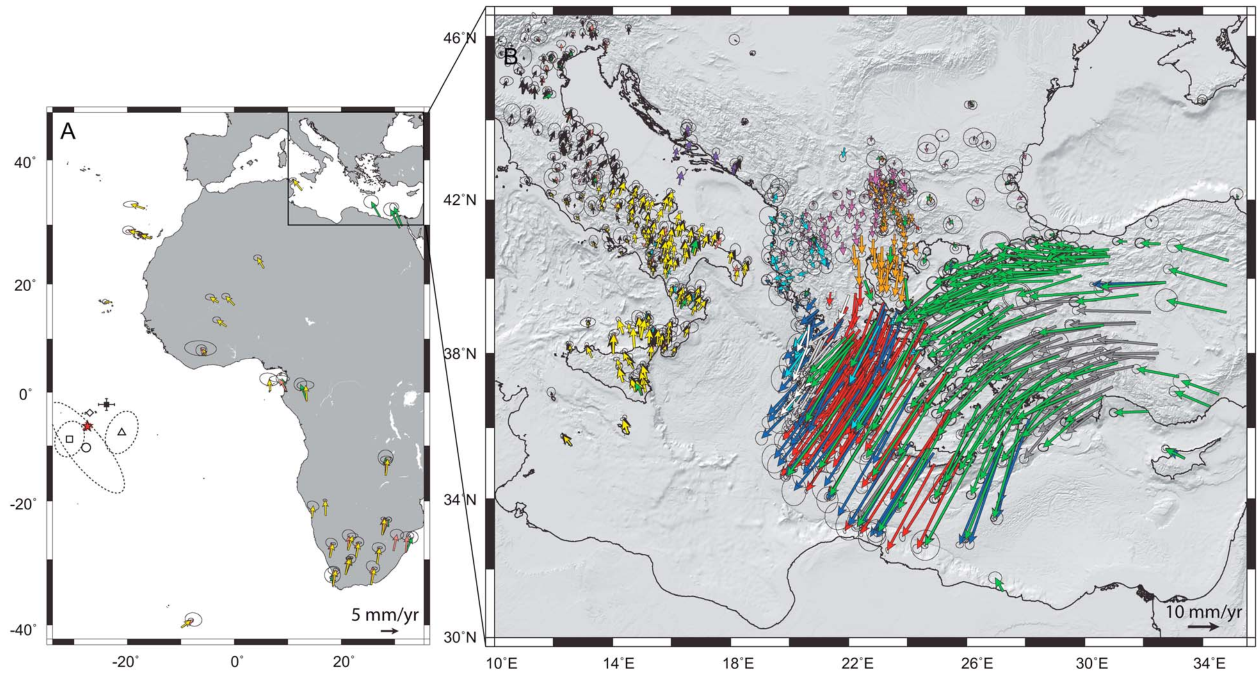


**Figure 2.** Input GPS velocities of the model. Velocities are in Eurasia fixed reference frame with their respective 95% confidence ellipse. Velocity vectors are color coded relative to the study they have been taken from: green, *Reilinger et al.* [2006]; dark gray, *Aktug et al.* [2009]; magenta, *Kotzev et al.* [2006]; orange, Matev et al. (manuscript in preparation, 2012); turquoise, *Jouanne et al.* [2012]; red, *Floyd et al.* [2010]; light gray, *Charara* [2010]; white, O. Charade and A. Ganas (permanent GPScope network, available at https://gpscope.dt.insu.cnrs.fr/chantiers/corinthe/); blue, *Hollenstein et al.* [2008]; coral, *D'Agostino et al.* [2008]; yellow, *D'Agostino et al.* [2011a]; purple, *Bennett et al.* [2008]; black, *Devoti et al.* [2011]. (a) GPS velocities of the entire Nubian plate used to constrain the Nubia–Eurasia relative motion. Nubia–Eurasia rotation pole defined in this and previous studies are shown with their 1$\sigma$ confidence ellipse: circle, *Calais et al.* [2003]; diamond, *Le Pichon and Kreemer* [2010]; open square, *D'Agostino et al.* [2008]; triangle, *Argus et al.* [2010]; filled square, *Reilinger et al.* [2006]; red star, present study. Parameters of these rotation poles are summarized in Table 2. (b) Focus on the GPS velocities in the Central and Eastern Mediterranean region.

*Sokoutis*, 2010], the Miocene Aegean extensional system may extends further north (Figure 1b). The E-W trending grabens of Central Bulgaria are proposed to be the northward limit of the Miocene Aegean extensional system, and would have initiated around 9 Ma [*Burchfiel et al.*, 2000].

[8] Ongoing subduction in the Eastern Mediterranean led to the collision of the Apulian platform against Albania and western Greece in Late Miocene-Early Pliocene. Continued subduction of the remnant oceanic Ionian lithosphere resulted in the formation of the dextral Kefalonia Fault to accommodate the transition from continental collision in Western Greece (west of the fault) to oceanic subduction below Peloponnesus (east of the fault) [*van Hinsbergen et al.*, 2006; *Brun and Sokoutis*, 2010; *Royden and Papanikolaou*, 2011]. Recent studies confirms that the crust of the lithosphere subducting below the Peloponnesus is thin (ca. 8 km [*Suckale et al.*, 2009]), suggesting an oceanic nature, whereas crustal thickness increases to 20 km northwest of the Kefalonia Fault below western Greece [*Pearce et al.*, 2012]. In western Anatolia, E-W steep normal faults of Pliocene age crosscut the older Early Miocene low-angle detachment fault in the Büyük Menderes and Gediz Grabens [*Yilmaz et al.*, 2000; *Bozkurt and Sozbilir*, 2004]. In the Balkans, activity of NW trending detachment fault in northern Greece-SW Bulgaria ceased after ~3.5 Ma [*Dinter and Royden*, 1993]. From that time, extension is purely N-S directed in western Bulgaria and Northern Greece, accommodated by E-W trending neo-formed or reactivated normal faults [*Burchfiel et al.*, 2008]. Right-lateral displacement along the North Anatolian Fault (NAF) started in Middle Miocene time in Eastern Anatolia (ca. 11–12 Ma [*Şengör et al.*, 2005]) and reached the north Aegean in Early Pliocene times (~5 Ma [*Armijo et al.*, 1999]). The NAF thus

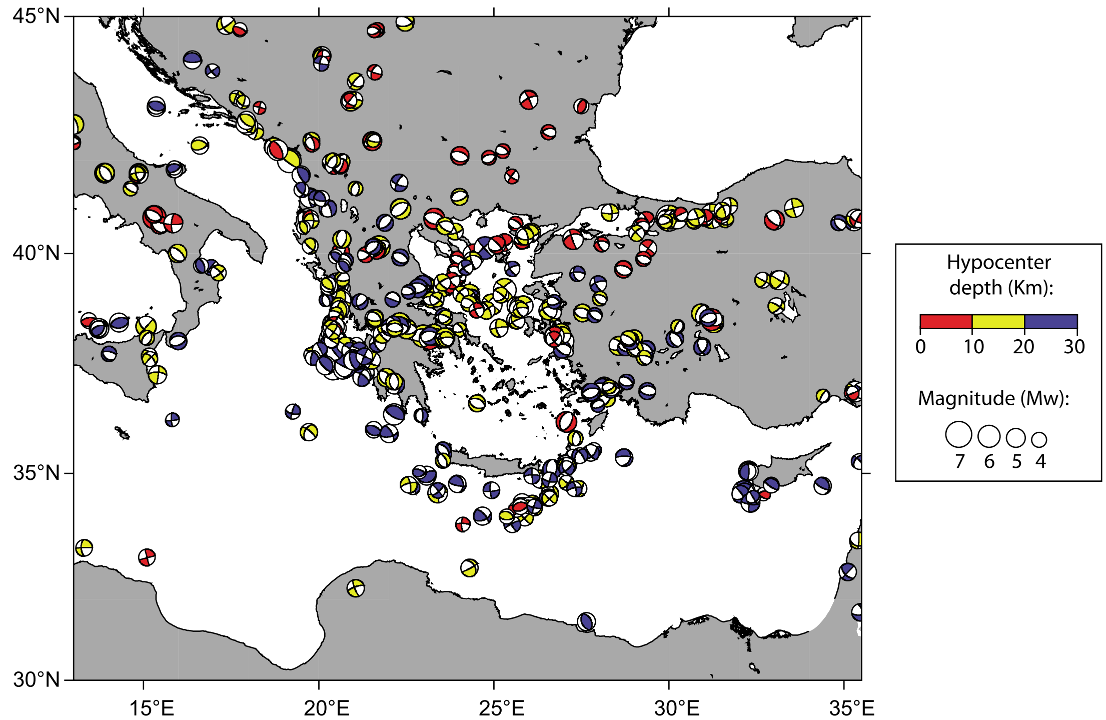


**Figure 3.** Input seismic moment tensors of the model. Fault plane solutions are from the Harvard CMT catalog (from 1976 to 2007) and the Regional Centroid Moment Tensor (RCMT) catalog (from 1995 to 2007). Location and hypocenter depth of the events are relocalized according to the *Engdahl et al.* [1998] catalog.

perturbed the continued extension in the Balkans and Aegean in Early Pliocene times, the Eastern Balkans becoming decoupled and isolated from the main Aegean extension system south of the NAF [*Burchfiel et al.*, 2008]. The main recent E-W trending extensional structure is the Gulf of Corinth in Western Greece which begun to rift in Early Pliocene age (~4 Ma [*Collier and Dart*, 1991]). Detailed stratigraphic studies of the Plio-Pleistocene infill of the basin document an increase of tectonic activity and narrowing of the Corinth rift in Early Pleistocene ages [*Rohais et al.*, 2007].

[9] Today, geodetic data document active N-S extension on both sides of the Aegean block, while the Aegean domain itself is not deforming anymore [e.g., *Le Pichon et al.*, 1995]. East, extension spreads over the entire western Anatolia (~20 mm/yr extension rate over the whole western Turkey [*Aktug et al.*, 2009]) and west, it is localized in the Gulf of Corinth (~15 mm/yr [*Briole et al.*, 2000]). Focal mechanisms distribution shows that N-S extension also occurs in northwestern Aegean Sea (Figure 3). Northeastern Aegean Sea is affected by dextral active strike-slip related to the NAF (~25 mm/yr [*McClusky et al.*, 2000]). In the Balkan Peninsula, geodetic data suggest small but still active N-S extension [*Burchfiel et al.*, 2006], emphasized by historic seismic activity in Bulgaria revealed by morphotectonic and paleoseismic studies [*Meyer et al.*, 2007]. High seismic activity and transpression on the active Kefalonia Fault is well documented [*Louvari et al.*, 1999].

## 2.2. Central Mediterranean

[10] The Calabrian slab started to retreat toward the south and east in late Oligocene, the remnant oceanic Ionian lithosphere being progressively consumed at the Calabrian subduction zone [e.g., *Faccenna et al.*, 2001, 2004]. This retreat was associated with widespread back-arc extension, successively opening the Liguro-Provencal basin from 30 to 35 to 15 Ma and the Tyrrhenian basin from 15 Ma to present-day [*Malinverno and Ryan*, 1986; *Faccenna et al.*, 2001]. During Miocene times, the eastward retreating trench reached the western border of the Apulian continent, causing shortening and forming the present-day Apennines. Trench retreat at the Calabria subduction has been active until very recent time, according to the latest pulse of Pliocene oceanic accretion in the Marsili

**Table 1.** Angular Velocities That Rotate Original Geodetic Studies Into a Self-Consistent Eurasian Reference Frame[a]

| | Lat. (°N) | Long. (°E) | ω Pole (°/Myr) | Number of Common Sites | Original RMS | RMS After Rotation |
|---|---|---|---|---|---|---|
| O. Charade and A. Ganas (permanent GPScope network, available at https://gpscope.dt.insu.cnrs.fr/chantiers/corinthe/) | 39.95 | 19.67 | 0.238 | 5 | 1.35 | 0.74 |
| *Charara* [2010] | 45.37 | 20.71 | 0.116 | 4 | 1.61 | 1.23 |
| *Floyd et al.* [2010] | 43.90 | 12.98 | 0.042 | 31 | 1.01 | 0.60 |
| *Hollenstein et al.* [2008] | 43.98 | 26.00 | 0.132 | 15 | 2.16 | 1.37 |

[a]Velocity vectors of the following studies are rotated in order to minimize the root-mean square (RMS) difference with velocities of *Reilinger et al.* [2006] used as the common reference frame.

and Vavilov basins, at high rates (~6 cm/yr [*Malinverno and Ryan*, 1986]). Back-arc extension behind the Calabria Arc has now stopped, or has been reduced below the detection level of GPS measurements [*D'Agostino et al.*, 2008]. Since the cessation of spreading in the Tyrrhenian Sea, slab retreat slowed down or stopped, and a new geodynamic setting was established, including collapse within the upper plate (Calabrian Arc [*D'Agostino et al.*, 2011a]), fragmentation of the remaining lower plate (oceanic Ionian Sea and margins [*D'Agostino et al.*, 2008] and re-activation of the Pelagian grabens [*Torelli et al.*, 1995]. The entire Central Mediterranean is now slowly deforming, the present-day strain rate field being dominated by the collapse of the Apennines [*D'Agostino et al.*, 2011b; *Devoti et al.*, 2011] along NW-SE trending large-scale normal faults attesting Holocene activity [*Palumbo et al.*, 2004].

## 3. Deriving Crustal Horizontal Velocity and Strain Rate Fields

### 3.1. Geodetic and Seismologic Input Data

[11] Many geodetic studies have been carried out during the last decades over the Central Mediterranean, the Eastern Mediterranean and the Balkans. The increasing number of permanent stations and a mean 10 years time span for temporary stations now allow for the derivation of a reliable velocity field, not only for plate-scale motion, but also for slowly deforming regions. Central to our analysis is a compilation of 1415 velocity vectors, measured either by our group [*Charara*, 2010; *Jouanne et al.*, 2012; Matev et al., manuscript in preparation, 2012] (see also O. Charade and A. Ganas, permanent GPScope network, available at https://gpscope.dt.insu.cnrs.fr/chantiers/corinthe/), or published by other groups (Figure 2): central Mediterranean [*Bennett et al.*, 2008; *D'Agostino et al.*, 2008, 2011a; *Devoti et al.*, 2011]; western Aegean [*Hollenstein et al.*, 2008; *Floyd et al.*, 2010], Southern Balkans [*Kotzev et al.*, 2006], eastern Aegean and Turkey [*Reilinger et al.*, 2006; *Aktug et al.*, 2009], whole Nubian plate [*Reilinger et al.*, 2006; *D'Agostino et al.*, 2008, 2011a].

[12] Each of these geodetic studies gives their velocity solution in their own Eurasian reference frame. Following *Kreemer et al.* [2003], we make the assumption that differences between reference frames consist solely in a rigid body rotation for regional studies. Since the velocities of *Reilinger et al.* [2006] are the most numerous and were computed with the longest time span, we chose their Eurasian reference frame as the frame of reference for the entire compilation. Root-mean square (RMS) differences at common sites have been computed for each possible pairs of studies (RMS table is available in the auxiliary material).[1] For each study, the rotation that minimizes the RMS difference with *Reilinger et al.* [2006] was determined, in order to rotate the velocity vectors to the common frame. For studies having an original RMS very small (<1.3 mm/yr) with *Reilinger et al.* [2006], no rotation could improve the RMS minimization (except for *Floyd et al.*'s [2010] study, see table in auxiliary material). These were thus maintained in their original Eurasian reference frame [*Bennett et al.*, 2008; *D'Agostino et al.*, 2008; *Aktug et al.*, 2009; *D'Agostino et al.*, 2011a; *Devoti et al.*, 2011; *Jouanne et al.*, 2012]. Other studies could not be rotated since there were not enough common sites with *Reilinger et al.* [2006] or the few common sites showed too large uncertainties to be reliable [*Kotzev et al.*, 2006; Matev et al., manuscript in preparation, 2012]. The angular rotation applied to each set of velocity vectors is given in Table 1.

[13] In combination with the geodetic measurements, we use moment tensors extracted from the Harvard Centroid Moment Tensor (Harvard CMT) catalog for events with magnitude >6.5, and from the Regional Centroid Moment Tensor (RCMT)

[1]Auxiliary materials are available in the HTML. doi:10.1029/2012GC004289.

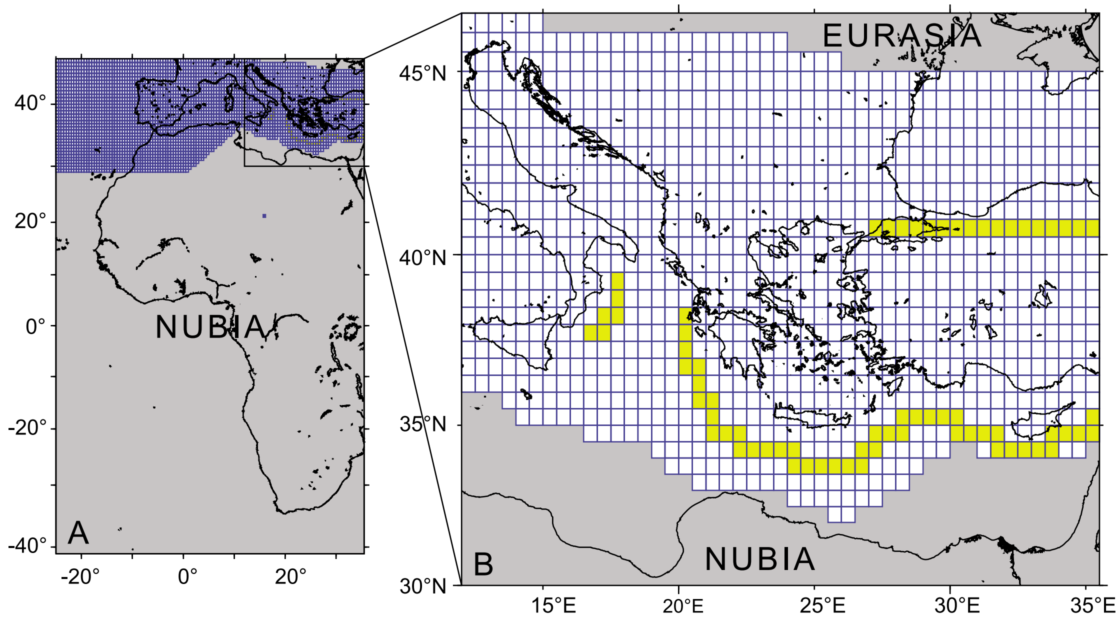


**Figure 4.** Presentation of the model. (a) The whole size of the box model and (b) a close-up of the model in the Mediterranean region. The model grid cells are 0.5° × 0.5° in dimension. Grey domains are not-allowed-to-deform cells ("rigid" cells), in order to mimic rigid tectonic plate. Cells outlined in blue are the deforming cells. The yellow cells are allowed to deform at a higher rate than the white ones.

catalog for events with magnitude comprised between 4.5 and 6.5. Duplicate between these two catalogs have been removed. We finally select 498 shallow events (≤30 km) which locations have been corrected using the Engdhal relocated catalog [*Engdahl et al.*, 1998]. The corresponding 498 focal mechanisms are plotted in Figure 3.

## 3.2. Description of the Model

[14] We use *Haines and Holt*'s [1993] method, which consists in deriving a continuous velocity and strain rate field by interpolating model velocities that are fitted in a least square sense to observed GPS velocities. To obtain this continuous velocity and strain rate field, we define a model grid of cells 0.5° by 0.5° in dimension. Cells located over stable Eurasian and Nubian plates are not allowed to deform in order to mimic rigid tectonic plates. All other cells, i.e., cells in the Mediterranean region, are free to deform (Figure 4). Strength anisotropy is introduced based on the focal mechanisms, where available. In this case, the direction of the strain rate field is controlled by the principal axis of deformation derived from seismic moment tensor of the Harvard CMT and RCMT catalog (note that only the direction of the strain rate field is constrained, not the sign of strain rate).

[15] The region covered by our model is much larger than our study area, since the modeled grid stretches from central Europe to South Africa and from western Morocco to eastern Cyprus (Figure 4). The advantage of a larger grid is twofold: edge effects are avoided and a self-consistent Nubia/Eurasia motion can be directly derived from the model, since three of the studies [*Reilinger et al.*, 2006; *D'Agostino et al.*, 2008, 2011a] include velocity vectors not only in the Mediterranean region, but also across whole Nubia. The Eurasia-Nubia rotation pole obtained in this study is defined in Table 2.

## 3.3. Long-Term Versus Transient Deformation

[16] Central and Eastern Mediterranean domains are subjected to blocks interactions [*D'Agostino et al.*, 2008] and/or diffuse deformation [*Floyd et al.*, 2010]. Our approach is to model the entire region using *Haines and Holt*'s [1993] method to derive a continuous velocity field without a priori statements on the geometry of rigid blocks [*Haines and Holt*, 1993]. We do not deny that these blocks may exist and that the GPS measurements close to the major faults contain a significant component of transient deformation such as interseismic loading and post-seismic relaxation. However, little information is available to map the boundaries of these blocks and even less to model the contact between them. Previous studies that have used *Haines and Holt*'s

**Table 2.** Rotation Poles of Plate Pairs Derived in This and Previous Studies[a]

| Plate Pair | Lat. (°N) | Long. (°E) | Ω (°.Myr$^{-1}$) | $\sigma_{maj}$ (deg) | $\sigma_{min}$ (deg) | Azimuth (deg) | σΩ (°.Myr$^{-1}$) | Reference |
|---|---|---|---|---|---|---|---|---|
| NU−EU | −7.5 | −21.1 | 0.061 | 4.2 | 2.7 | 25.0 | 0.009 | *Argus et al.* [2010] |
| NU−EU | −3.9 | −27.1 | 0.049 | 1.4 | 0.2 | 84.1 | 0.002 | *Le Pichon and Kreemer* [2010] |
| NU−EU | −8.7 | −30.8 | 0.049 | 3.4 | 2.6 | 22.4 | 0.001 | *D'Agostino et al.* [2008] |
| NU−EU | −2.3 | −23.9 | 0.059 | see note[b] | see note[b] | see note[b] | 0.001 | *Reilinger et al.* [2006] |
| NU−EU | −10.3 | −27.7 | 0.063 | 10.3 | 3.3 | 142.0 | 0.004 | *Calais et al.* [2003] |
| NU−EU | −6.4 | −27.5 | 0.051 | 0.7 | 0.7 | 74.15 | 0.001 | this study |
| AP−EU | 38.6 | 26.4 | −0.299 | 3.1 | 0.3 | −72.3 | 0.088 | *D'Agostino et al.* [2008] |
| (AP-IO)−EU | 38.7 | 26.8 | −0.272 | 0.8 | 0.3 | −86.6 | 0.018 | this study |
| AP−NU | 34.3 | 17.4 | −0.318 | 2.5 | 0.3 | −3.0 | 0.088 | *D'Agostino et al.* [2008] |
| (Ap-Hy)−NU | 33.0 | 17.5 | −0.265 | 1.7 | 0.3 | −5.1 | 0.041 | *D'Agostino et al.* [2008] |
| (AP-IO)−NU | 33.8 | 17.1 | −0.295 | 0.5 | 0.2 | −4.1 | 0.018 | this study |

[a]Angular velocities are for the first plate relative to the second. NU: Nubia; EU: Eurasia; Ap: "Apulian Block" defined by *D'Agostino et al.* [2008]; AP-IO: Apulian-Ionian block defined in this present study; (Ap-Hy): Block containing Apulia and Hyblean plateau in *D'Agostino et al.* [2008]. $\sigma_{maj}$ and $\sigma_{min}$ are the length in degrees of the semi-major and semi-minor axes of the 2-D 1$\sigma$ error ellipse, with the azimuth of the semi-major axis given clockwise from the north.

[b]NU/EU rotation pole parameters are given differently in *Reilinger et al.* [2006]: $\sigma_{lat}$ (deg): 1.1; $\sigma_{long}$ (deg): 1.5.

[1993] method have shown the possibility to distinguish a posteriori whether an area is moving as a rigid block or is affected by diffuse deformation [*Kreemer and Chamot-Rooke*, 2004]. Inter-seismic and post-seismic effects are thus included in the continuous velocity field that we derive, and it may thus be difficult to separate them from the long-term velocities. We however argue that long-term (i.e., steady state) motions dominate our velocity field. The inter-seismic loading at the North Anatolian Fault, for example, is restricted to the vicinity of the fault: 50 km on both sides of the fault translate to two nodes maximum in our model. Coupling immediately above the subductions may potentially induce deformation at larger distances, but the Hellenic subduction seems to be largely un-coupled, except perhaps in the vicinity of the Kefalonia Fault. Finally, no great earthquake (Mw > 8) broke the Calabria or Hellenic subduction plane during the last centuries, so that large-scale post-seismic effect can be excluded.

## 3.4. Homogeneous Versus Heterogeneous Runs

[17] As the model is purely kinematic, rigidity is not included *sensu stricto*. However, a cell strength parameter that controls the ability of cells to deform is introduced through the use of isotropic strain rate variances [see *Haines and Holt*, 1993]. Strength can be uniform – all cells deform equally – or non-uniform if some cells are allowed to strain at higher rates in the process of fitting observed velocities [*Beavan and Haines*, 2001].

[18] The core of the results presented is based on heterogeneous models (non-uniform cell strength), but results for uniform cells strength are available in the auxiliary material, for comparison. The advantage of the heterogeneous models is to allow for strain localization on some of the main tectonic boundaries. In order to keep the model as simple as possible (and reduce a priori assumptions), we choose to perform runs with uniform cell strength throughout the deforming grid, except along three weak areas (Figure 4). The first weak area is along the North Anatolian Fault. The fault system is well established in the field, underlined by a narrow band of seismicity and punctuated by high magnitude earthquakes. The North Anatolian Fault is thus seen as a mature plate boundary where strain is localized. The second and third weak areas are respectively along the Hellenic subduction zone and the Calabrian subduction zone. Again, to keep the model simple, we do not take into account the deformation within the accretionary prisms, i.e., the Calabrian prism and the Mediterranean Ridge. Weak areas are however placed in the region of transition from the wedges to the backstops, both on the Calabrian and Hellenic sides. Details of the accommodation of the Nubia-Aegean convergence within the Mediterranean Ridge can be found in the study of *Kreemer and Chamot-Rooke* [2004]. The Kefalonia Fault zone, which is a mature fault system at the northwestern termination of the Hellenic subduction zone, is also modeled as a weak area.

# 4. Results

[19] The obtained velocity field is plotted by default in the same reference frame than that of the input GPS data, i.e., the Eurasia fixed reference frame (Figure 7). Second invariant strain rate and strain

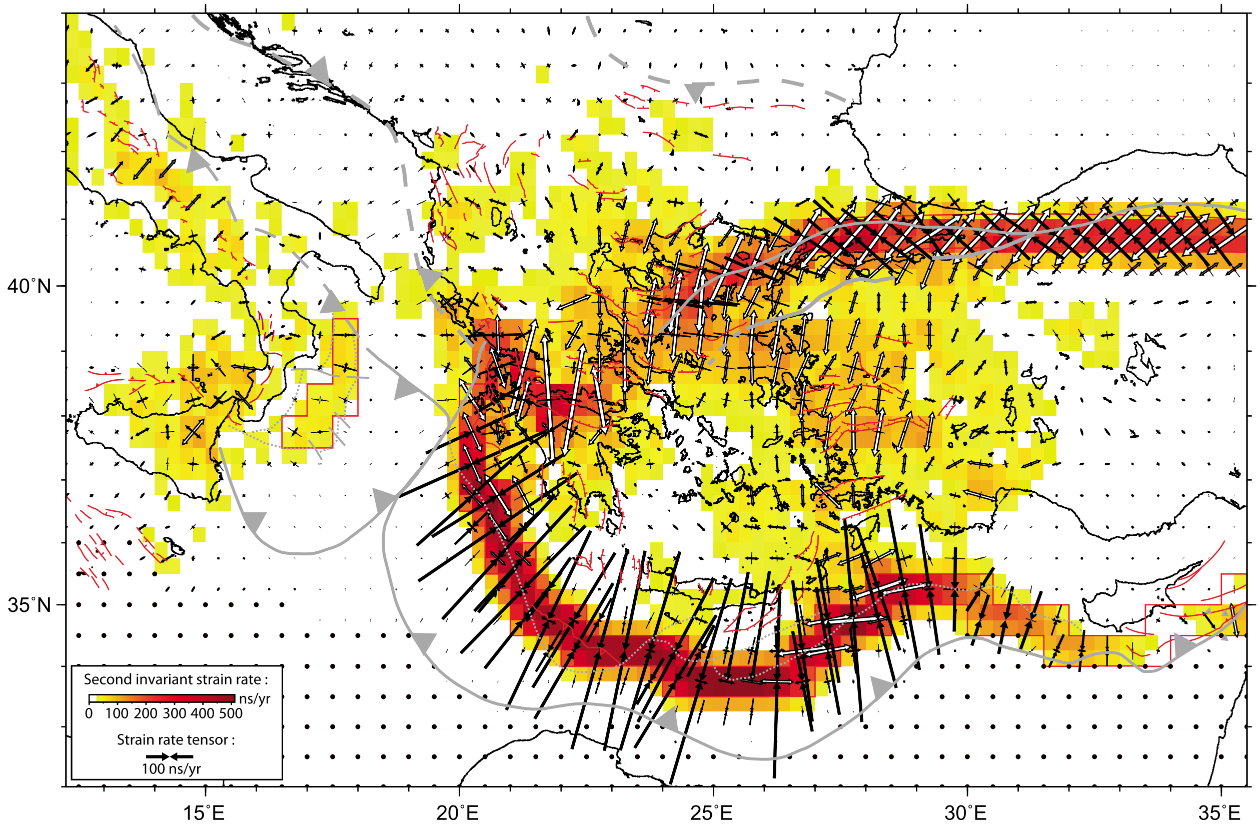


**Figure 5.** Strain map of the Central and Eastern Mediterranean (i.e., second invariant strain rate and strain rate tensors). The second invariant of horizontal strain represents the "magnitude" of strain and is defined as $\sqrt{(\varepsilon_{xx}^2 + \varepsilon_{yy}^2 + 2.\varepsilon_{xy}^2)}$ where $\varepsilon_{xx}$, $\varepsilon_{yy}$, $\varepsilon_{xy}$ are the horizontal components of strain rate tensor. Strain unit "ns/yr" is nanostrain/year ($10^{-9}$/ yr). Major tectonic structures are plotted in gray. Also superimposed are active faults in red (seismic and/or Holocene activity), compiled from various studies [*Benedetti*, 1999; *Bozkurt and Sozbilir*, 2004; *Palumbo et al.*, 2004; *Chamot-Rooke et al.*, 2005; *Papanikolaou et al.*, 2006; *Burchfiel et al.*, 2008]. Black dots are the nodes of the "rigid" Nubia cells (see Figure 4).

rate tensors derived from the model are plotted in Figure 5. The second invariant was split into its dilatational component and maximal shear component (Figures 6a and 6b). We briefly outline in this section the main characteristics of the modeled field, region by region.

### 4.1. Anatolia-Aegean Domain

[20] The velocity field that we obtain in the Anatolia-Aegean domain is similar to the solutions discussed in many previous studies [*McClusky et al.*, 2000; *Reilinger et al.*, 2006; *Floyd et al.*, 2010; *Le Pichon and Kreemer*, 2010]. We emphasize here some of the elements that will become important in the discussion. Anatolia-Aegean domain is characterized by a circular counter-clockwise motion relative to Eurasia (Figure 7): velocities are ~2 cm/ yr, W directed, in eastern Anatolia and reach ~3 cm/yr, SW directed in Aegean. This domain is bounded to the north by the North Anatolian Fault (NAF), Eurasia-Anatolia plate boundary, which shows an expected strike-slip behavior with high value of second invariant strain rate of 300–400 ns/yr (nanostrain/year=$10^{-9}$/year, Figures 5 and 6). The westward limit of high values of shear component is located in the North Aegean Trough south of the Thessaloniki Peninsula (long. 24°E; lat. 39.75°N). Strain localizes along the NAF, even if weak cells along the fault are not included (see the homogeneous run in the auxiliary material). The southern boundary of Anatolian-Aegean domain is the Hellenic and Cyprus subduction zones (backstop front). In addition to a main compressional component, the Hellenic subduction shows a substantiate amount of shear component along the western and eastern Hellenic fronts (respectively dextral and sinistral), except in southwestern Crete where strain is purely compressional (Figure 6). Furthermore, the relative plate motions at the Hellenic trench calculated with our modeled velocities show a relative convergence

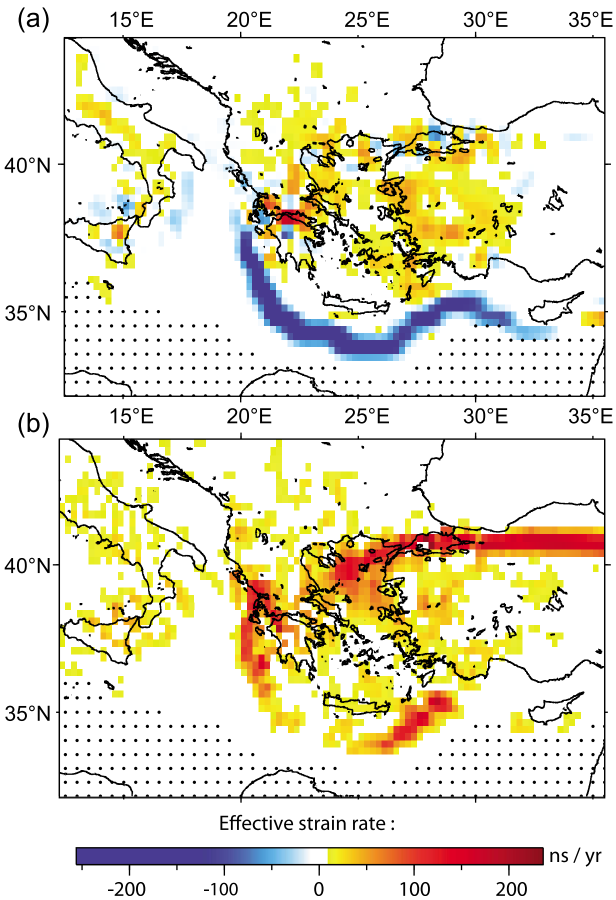


**Figure 6.** (a) Dilatational strain rate ($\sigma$). Dilatation is positive, compression is negative. (b) Maximal shear strain rate ($\gamma_{max}$). $\sigma$ and $\gamma_{max}$ are defined as: $\sigma = 0.5 (\varepsilon_{xx} + \varepsilon_{yy})$ and $\gamma_{max} = \sqrt{[(0.5(\varepsilon_{xx} - \varepsilon_{yy}))^2 + \varepsilon_{xy}^2]}$ where $\varepsilon_{xx}$, $\varepsilon_{yy}$, $\varepsilon_{xy}$ are the horizontal components of strain rate tensor. Black dots are the nodes of the "rigid" Nubia cells (see Figure 4).

direction that is not perpendicular to the direction of the Hellenic trench (Figure 13). Those elements are in agreement with occurrence of strain partitioning along the Hellenic subduction zone due to the oblique relative convergence between Nubia and the Aegean domain [*Le Pichon et al.*, 1995; *Kreemer and Chamot-Rooke*, 2004].

[21] Eastern Anatolia and central-southwestern Aegean are the only regions that seem to behave rigidly (Figure 5), in agreement with results of previous studies [*Kahle et al.*, 1999; *McClusky et al.*, 2000; *Kreemer and Chamot-Rooke*, 2004; *Reilinger et al.*, 2006; *Le Pichon and Kreemer*, 2010]. The remaining areas are affected by localized N-S directed extension in the Gulf of Corinth and diffuse N-S extension spread over western Turkey and eastern Aegean Sea [*Briole et al.*, 2000; *Jolivet*, 2001; *Aktug et al.*, 2009]. Values of strain rate are high in the Gulf of Corinth (~300 ns/yr) and comprised between 50 ns/yr and 180 ns/yr in western Turkey.

## 4.2. Southern Balkans

[22] Our study suggests that the Balkans do not belong to stable Eurasia, a result that is central to our interpretation. South directed residuals (>1 mm/yr) relative to Eurasia become significant south of the latitude 43°N and gradually increase southward (Figure 7). In the eastern Balkans, those residuals are small (1 to 3 mm/yr) and the second invariant suggests that the area is either rigid, or very slowly straining. On the contrary, Southern Balkans (Macedonia and western Bulgaria), Albania and continental Greece are affected by diffuse deformation with strain rate values comprised between 50 ns/yr and 150 ns/yr (Figure 5). As noticed in previous studies [*Burchfiel et al.*, 2006; *Kotzev et al.*, 2006], our model emphasizes the complexity of active strain in this region: from west to east, strain rate tensors show strike-slip along the Albanian coast; E-W directed extension in Macedonia and distributed N-S directed extension from western Bulgaria to northern Greece. However, distributed N-S extension is not limited to the Southern Balkans, but is actually spreading and increasing further south, and reaches the eastern Gulf of Corinth (Figure 5). The entire area of diffuse deformation in Albania-Southern Balkans-continental Greece has a significant southward motion relative to Eurasia where a double gradient of motion occurs: the velocities are increasing from west to east (Figure 7, long. 21°E to 24°E); the velocities are increasing from north to south starting from 1.5 mm/yr near the Sofia graben (lat. 43°N) and gradually reaching 11 mm/yr in the N Aegean (lat. 40°N). From this point, the velocities vectors gradually rotate clockwise and increase to reach ~30 mm/yr, SW directed, at the eastern Gulf of Corinth.

## 4.3. Central Mediterranean

[23] The Ionian Basin, the Hyblean plateau (Miocene nappes and platform of Sicily), the Apulia Peninsula and the Adriatic Sea are behaving rigidly (Figure 5). Relative motions in the Ionian/Calabrian region cannot be straightforward evidenced in a fixed Eurasia or Nubian reference frame, as noticed by *D'Agostino et al.* [2008]. In this reference frame, the Nubian plate is moving toward the NW, the Tyrrhenian Sea is moving toward the North and the

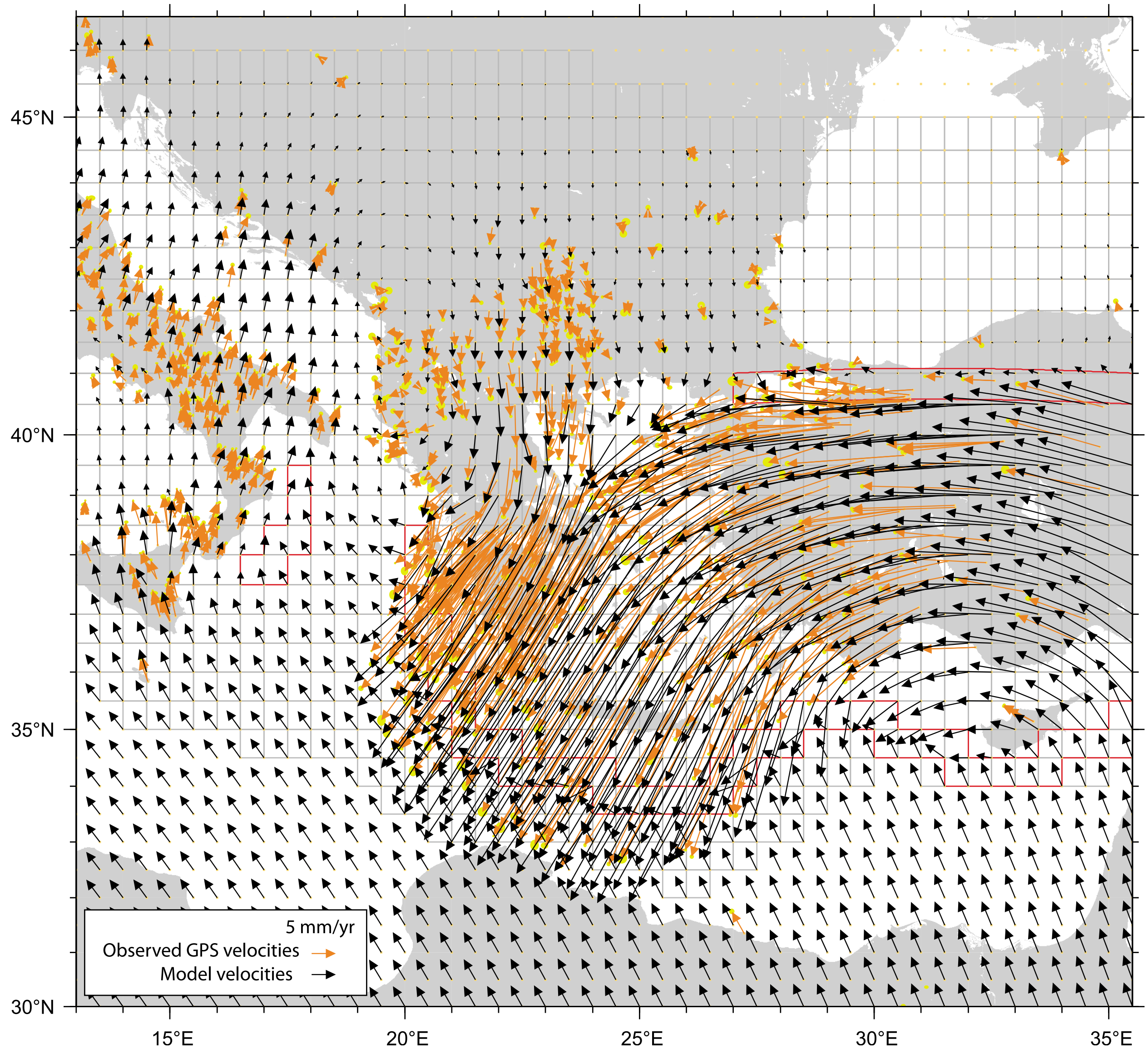


**Figure 7.** Observed and interpolated model velocities with respect to Eurasia. Red polygons outline the weak cells areas defined in the model.

Adriatic platform is moving toward the NE (Figure 7). Following *D'Agostino et al.* [2008], we minimize velocity vectors of the Hyblean plateau and Apulia Peninsula to derive a rigid rotation pole for an Apulian-Ionian block. We find that the rigid rotation that minimizes (residuals <1 mm/yr) the Hyblean plateau and the Apulia Peninsula actually minimizes model velocities of a much larger area, including the Ionian Basin, the south Adriatic Sea, the Sirte Basin and its margins toward Libya (Figure 8). We call the minimized area "Apulian-Ionian block." Significant motion occurs in Eurasia, Nubia, the North Adriatic Sea, the Tyrrhenian Sea and Calabria relative the fixed Apulian-Ionian block reference frame.

[24] To constrain the possible spatial extent of the Nubian plate in Central Mediterranean, we show in Figure 9 grid notches that have velocities less 1 mm/yr in Nubia fixed reference frame (modeled velocity field relative to Nubia is available in the auxiliary material). Combining the rotation pole of the Apulian-Ionian block relative to Eurasia with the Nubia-Eurasia pole, we derive the rotation pole of the Apulian-Ionian block with respect to Nubia, which is located in the Sirte plain (Figures 8 and 9). Parameters of the rotation poles of Apulian-Ionian block relative to Eurasia and Nubia defined in this study are given in Table 2. Not surprisingly, we find rotation poles parameters very close to those of *D'Agostino et al.* [2008] as we minimized motions

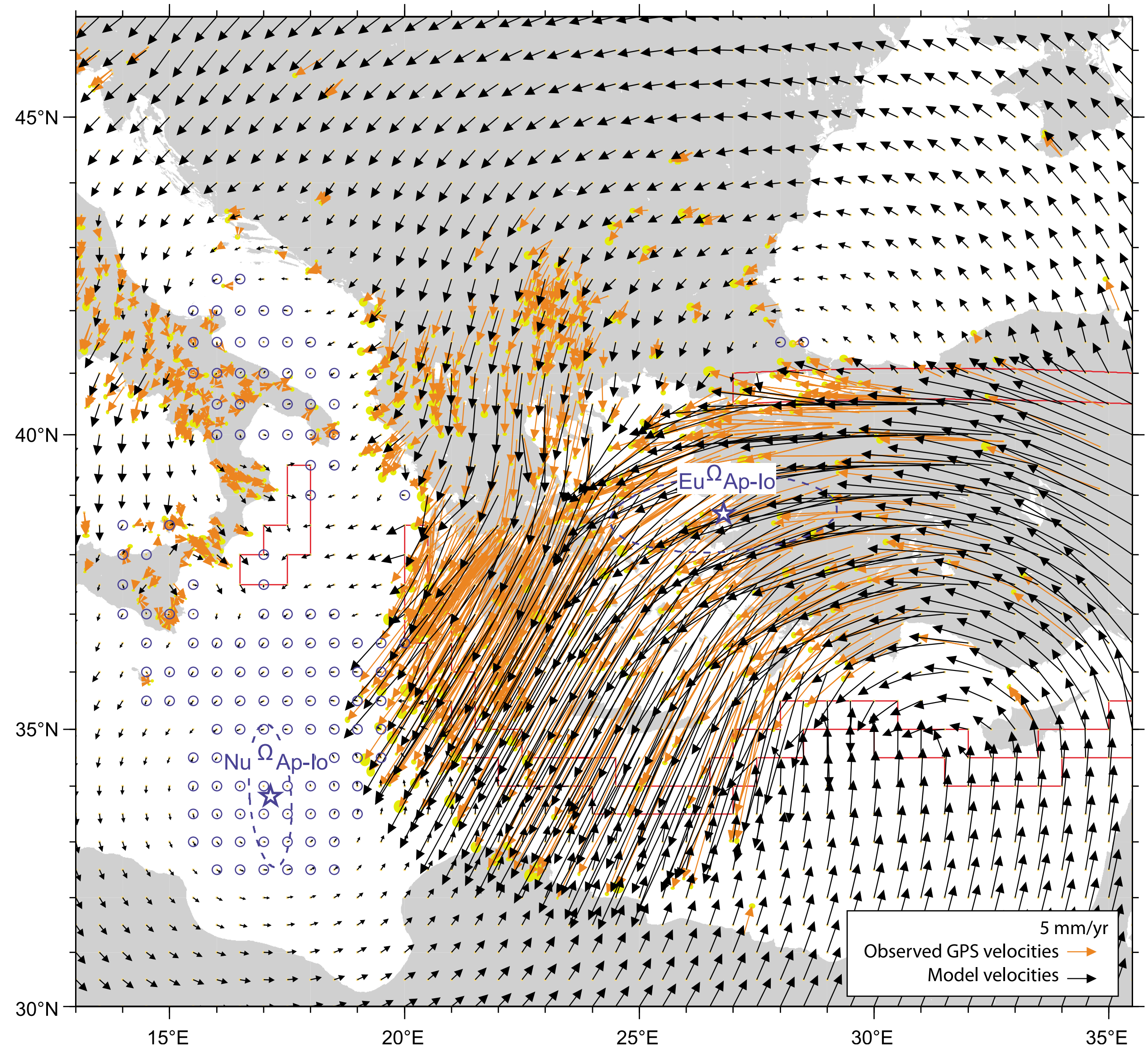


**Figure 8.** Observed and interpolated model velocities in the fixed Apulian-Ionian block reference frame defined in this study. Grid notches circled in blue have velocities <1 mm/yr in this reference frame. Rotation pole of this Apulian-Ionian block relative to Eurasia (Eu $^{\Omega}$Ap-Io) and to Nubia (Nu $^{\Omega}$Ap-Io) are shown with their 95% confidence ellipse. Parameters of these Eulerian poles are given in Table 2.

in the same regions to determine the Eurasia/Apulian-Ionian block rotation pole.

[25] Deformation starts to be significant in NW Albania with a high oblique convergence, NNE-SSW directed, of ~4 mm/yr. Further south, along the western Greece coast, the convergence turns to pure frontal with value of ~5 mm/yr (Figures 5 and 9). A jump of convergence rate occurs southeast of the Kefalonia Fault to reach 34 mm/yr in Southern Greece. A NE-SW extension of ~2.2 mm/ yr occurs south of the Apulian-Ionian block in the Pelagian Sea. The Calabria Arc has a small trenchward motion with respect to the Apulian-Ionian block, of the order of 2–2.5 mm/yr whereas compression occurs north of Sicily (strain rate values around 50 ns/yr). Finally, localized SW-NE directed extension of 4–5 mm/yr occurs along the Apennines chain with strain rate value around 100 ns/yr (Figure 5), consistent with the values of *Devoti et al.* [2011].

## 4.4. Absolute Plate Motions

[26] One way to examine the relationship between crustal motions and hypothetic mantle flows is to use the Absolute Plate Motion (APM) reference

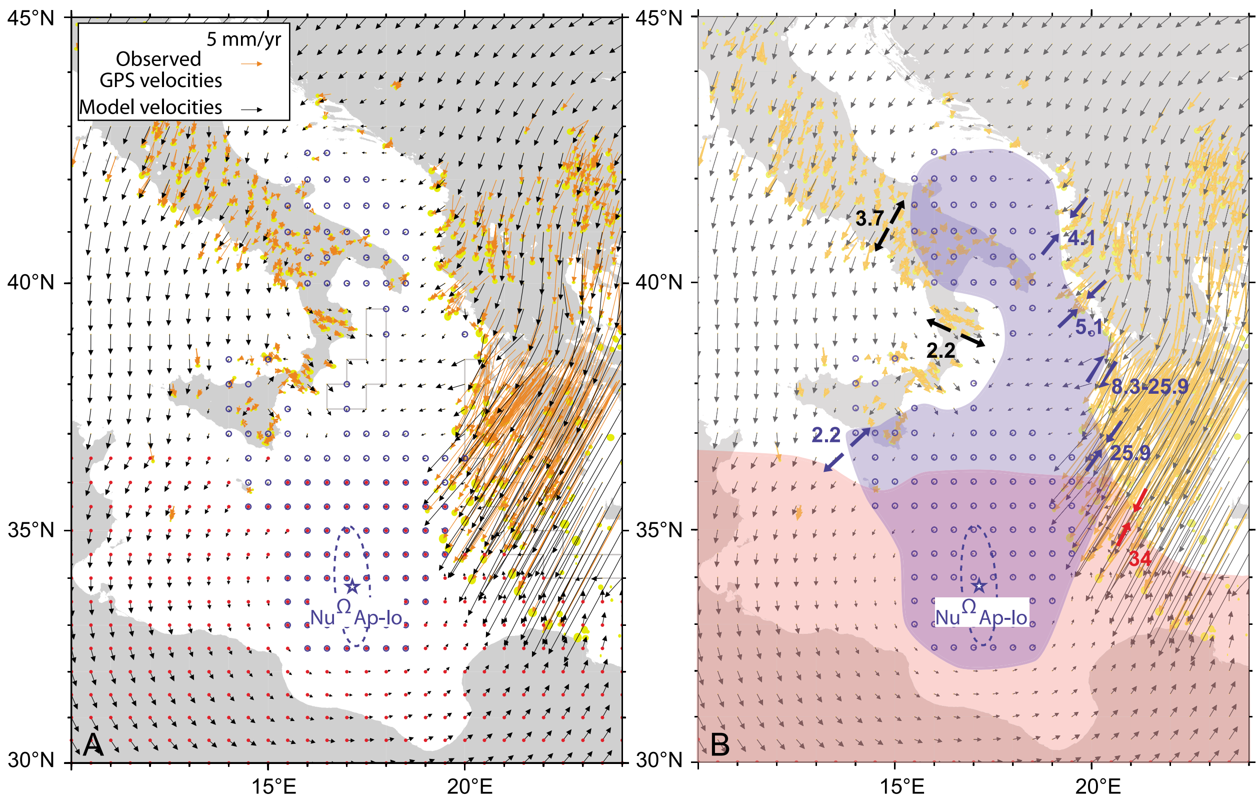


**Figure 9.** (a) Close-up of the observed and interpolated model velocities with respect to the Apulian-Ionian block. Grid notches circled in blue: velocities <1 mm/yr in this reference frame; grid notches circled in red: velocities <1 mm/yr in fixed Nubia reference frame. (b) Kinematic sketch of the Central Mediterranean. Cells within the blue domain have small residuals with respect to the Apulian-Ionian block, whereas cells within the red domain have small residuals with respect to Nubia. Relative motions have been measured at the boundaries of the Apulian-Ionian block (blue arrows), Nubian plate (red arrows) and in internal Apennines and Calabria (black arrows). Boundaries of these domains should not be taken as true tectonic boundaries: they simply help in defining regions that are kinematically undistinguishable, at the 1 mm/yr level, from the Apulian-Ionian block and/or Nubia.

frame. APM reference frames based on hot spot track data like the HS3-NUVEL1A [*Gripp and Gordon*, 2002] are well adapted for fast-moving plates containing reliable hot spot tracks data, but errors are large on the motion of slow moving plates such as Nubia, Eurasia and Antarctica. We thus chose the absolute plate motion reference frame GSRM-APM-1 defined by *Kreemer* [2009] in which the motion of the slow-moving Nubian and Eurasian plates are constrained by the orientation of SKS share wave splitting observation from oceanic islands and cratons. Net rotation of the entire lithosphere relative to the lower mantle induces a shear component on upper mantle deformation. *Becker* [2008] shown that the amount of net rotation has to be moderate (~50% of HS3-NUVEL1A) to match global azimuthal anisotropy. GSRM-APM-1 predicts a net rotation which is about half of the HS3-NUVEL1A [*Kreemer*, 2009], suggesting that the GSRM model may be more appropriate to discuss APM and seismic anisotropy directions in further sections.

[27] In the GSRM-APM-1 absolute plate motion reference frame, Nubian and Eurasian plates are moving together toward the NE (Figure 10): motions are 11 mm/yr NNE directed for the Nubian plate and 6.5 mm/yr NE directed for the Eurasian plate. The most striking properties of the modeled velocity field are the twin toroïdal patterns found at both ends of the Hellenic subduction zone (Figure 10). Anatolia and Aegean follow a counterclockwise circular motion with an approximate radius of 500 km centered on the eastern end of the Hellenic subduction zone, while Northern and Western Greece show a clockwise circular motion with a radius of ~200 km centered on the western ending region of the Hellenic subduction zone. The centers of these toroïdal cells are shown as red dots in Figure 10. The eastern toroïdal flow has previously been discussed in *Le Pichon and Kreemer*

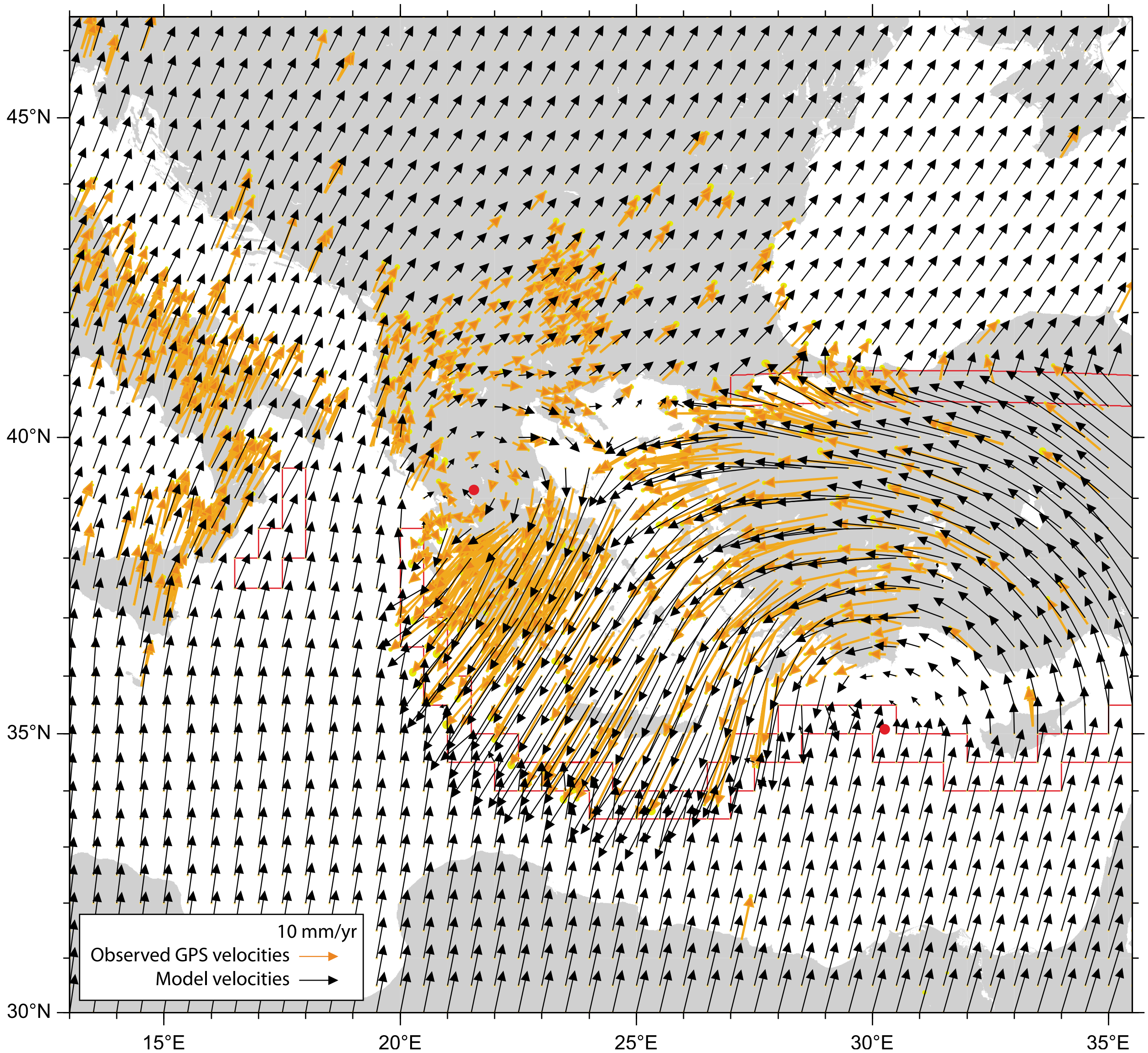


**Figure 10.** Observed and interpolated model velocities in absolute plate motion (APM) reference frame (GSRM-APM-1, reference frame defined by *Kreemer* [2009]). The red dots locate the centers of the two surface toroïdal patterns, which are located at both ends of the Hellenic subduction zone.

[2010] and interpreted as the result of mantle flow in the vicinity of a slab tear [*Govers and Wortel*, 2005; *Faccenna et al.*, 2006; *Keskin*, 2007].

## 5. Discussion

### 5.1. Extension in the Southern Balkans and the Western Termination of the North Anatolian Fault (NAF)

[28] A clear output of our model is that the Southern Balkans move southward with respect to Eurasia. This was suggested by previous studies [*Burchfiel et al.*, 2006; Matev et al., manuscript in preparation, 2012], but our results, combined with morphological and tectonic evidences, allows discussing the relationship between the Southern Balkans kinematics and the supposed westward propagation of the NAF throughout the entire northern Aegean Sea.

[29] In the north Aegean, our results demonstrate a lateral variation of the velocity and strain rate field from east to west. Other features such as bathymetry, fault network geometry of the NAF and focal mechanism are also evolving from east to west, depicting three main areas (Figure 11c): (1) In NW Turkey (east of the longitude 25°E), the NAF has a

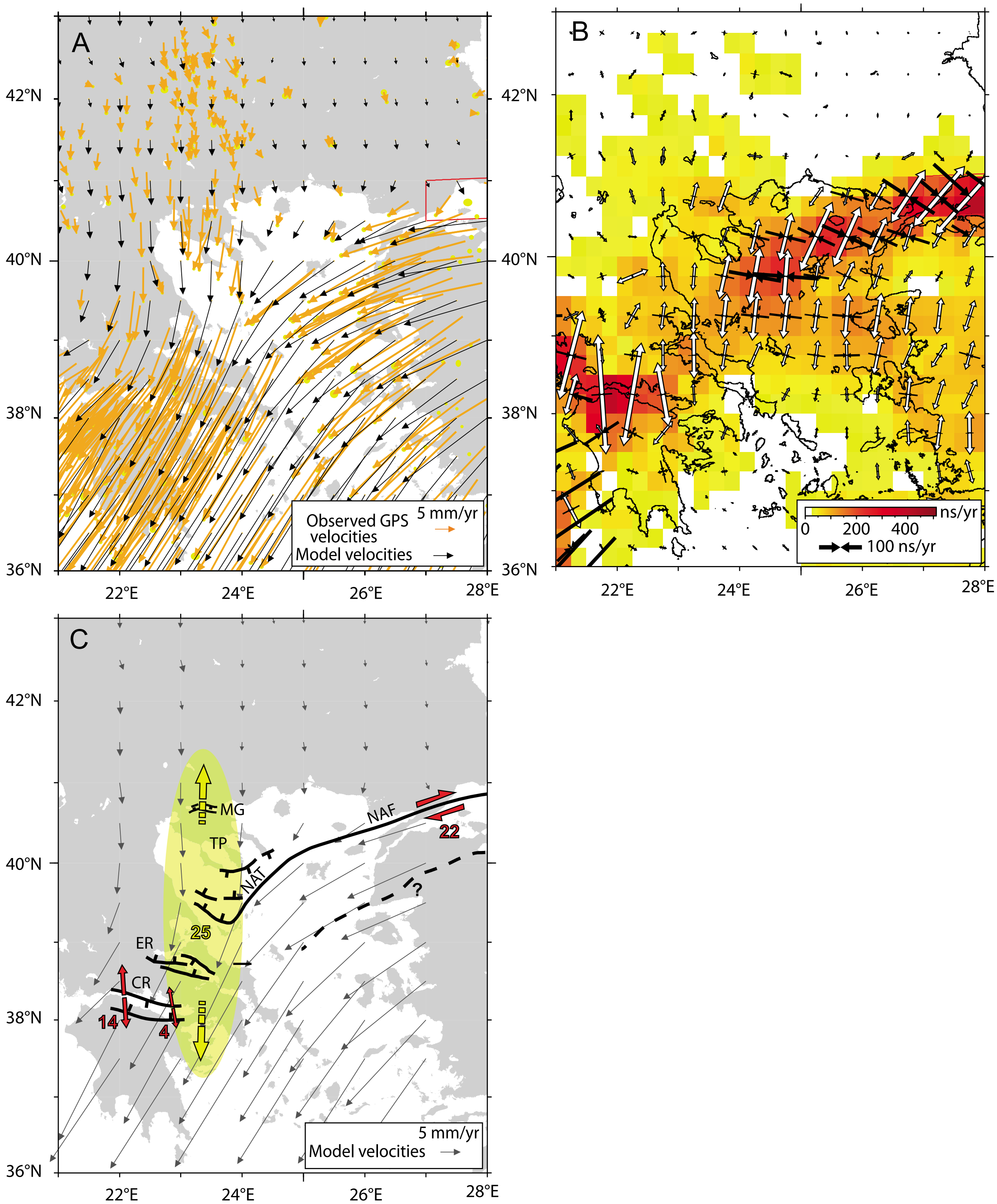


**Figure 11.** (a and b) Extracted from Figures 7 and 5 respectively. (c) Sketch showing the kinematic and tectonic junction between Anatolia, the Southern Balkans and western Aegean. Faults in the North Aegean Trough are from *Papanikolaou et al.* [2006]. Red arrows are the relative motions accommodated by localize strain across the NAF and the Corinth Rift (CR); yellow ellipse and yellow arrows emphasize the distributed N-S extension over the Southern Balkans and western Aegean. MG: Mygdonian graben; TP: Thessaloniki Peninsula; NAT: North Aegean Trough; ER: Evia Rift.

ENE-WSW direction and major localized dextral strike-slip accommodate the relative motions between the slowly moving Eastern Balkans and the fast westward moving Anatolia-Aegean domain (∼22 mm/yr relative to Eurasia); (2) When southward motion increases in the Balkans (between the longitude 25°E and 24°E), the strain regime along the NAF becomes transtensional as revealed by strain rate tensors and the occurrence of both strike-slip and extensional focal mechanisms (Figures 3, 11a, and 11b). Coherently, the direction of the NAF segments turns from ENE-WSW to NE-SW and are associated with a transtensional related basin, the north Aegean trough [e.g., *Papanikolaou et al.*, 2006]; (3) West of the longitude 24°E, southward motion becomes significant (∼10–11 mm/yr) so that the relative motion between the Balkans and Central Aegean is accommodated by distributed N-S directed extension spreading from eastern Macedonia-SW Bulgaria to the eastern Gulf of Corinth (Figures 11a and 11b). Potential structures accommodating this N-S directed extension are E-W trending normal fault distributed over Southern Balkans and western Aegean, which show morphological evidences for Quaternary activity and historic or present-day seismicity: the Kocani-Kruptnik-Bansko faults system [*Meyer et al.*, 2007], Mygdonian graben [e.g., *Stiros and Drakos*, 2000], the Evia rift and the eastern Corinth rift (Figures 3 and 11c). The NE-SW directed dextral segments of the North Aegean Trough terminate into spoon shaped E-W trending normal faults (Figure 11c).

[30] Kinematically, the net result is that in the north Aegean, we find no evidence for a high shear component west of the Thessaloniki Peninsula (longitude 24°E, Figure 11b), as would be expected if the NAF was crossing the Aegean Sea and reaching the eastern Gulf of Corinth as proposed by many studies [*Armijo et al.*, 1996; *Goldsworthy et al.*, 2002; *Flerit et al.*, 2004; *Reilinger et al.*, 2010; *Shaw and Jackson*, 2010]. Extension occurs on both the northern side and the southern side of the western tip of the NAF (Figure 11b). In other words, the relative motion between stable Eurasia and western Aegean domain is gradually accommodated by distributed N-S extension, so that the propagation of the NAF throughout continental Greece or Peloponnesus is not required (Figure 11c). In addition, the east to west fault network geometry evolution of the NAF in the north Aegean can be interpreted as the transition from strike-slip fault system to normal faults system in response to lateral variations of the kinematic boundary conditions. We thus locate the western termination of the dextral NAF south of the Thessaloniki Peninsula where the fault system turns into spoon-shaped E-W normal faults (Figure 11c).

[31] The velocity field with respect to Eurasia further shows that the motion of Southern Balkans is diffuse. Velocities are increasing southward in a ∼300 km wide corridor, from W Albania, N Bulgaria to Eastern Gulf of Corinth (Figure 7 or 11a). The entire Southern Balkans thus seem to be spreading southward, in a flow-like pattern. This flow-like pattern is clearly toroïdal in the APM reference frame (Figure 10). Southward spreading and flow-like pattern affecting the Southern Balkans may be driven either by lateral drag in response to the SW motion of the Aegean domain (sometimes referred as the Central Hellenic Shear Zone), horizontal gradient of gravitational potential energy [*Floyd et al.*, 2010; *Özeren and Holt*, 2010], flow located in the ductile lower crust (analogous to crustal channel flows models proposed for eastern Himalaya [*Beaumont et al.*, 2004]) or flow located deeper in the asthenosphere. Whatever the depth of the flow, it seems to be associated with the retreating Hellenic slab. If the correct interpretation is flow in the asthenosphere, it needs to be transferred to the crust. Recent numerical modeling studies investigated the viscous coupling at the lithosphere-asthenosphere boundary and have shown that in some cases, plates motion can be driven by basal drag from strong asthenospheric flow [*Hoink et al.*, 2011]. Basal traction related to asthenospheric flow is also proposed to contribute to continental domains motions, in the light of geological or seismic anisotropy arguments [*Alvarez*, 1990, 2010; *Bokelmann*, 2002; *Jolivet et al.*, 2008]. Surface flow would mimic a deeper asthenospheric flow associated with the “feeding” of the fast retreating Hellenic slab. The possibility of flow related to a slab break-off is discussed in a further section.

[32] Whatever the mechanism at work, lithospheric side drag or lower crust/asthenospheric flow, the main consequence of the southward motion of the Southern Balkans is the termination of the localized shear along the NAF in the North Aegean, south of the Thessaloniki Peninsula: extension in the Balkans de-activates the tip of the NAF. This extension ultimately leads to the opening of the Corinth Gulf: north of the Corinth Gulf, motion is increasing eastward, whereas south of the Gulf, the entire Peloponnesus is moving SW at a constant velocity. The net effect is a westward increase of the opening rate in the Gulf of Corinth, from 4 mm/yr to 14 mm/yr (Figure 11c). Locally, at the scale of the Corinth Gulf, our model is kinematically not different from the blocks model proposed by *Goldsworthy et al.* [2002] or *Shaw and Jackson* [2010]. The main

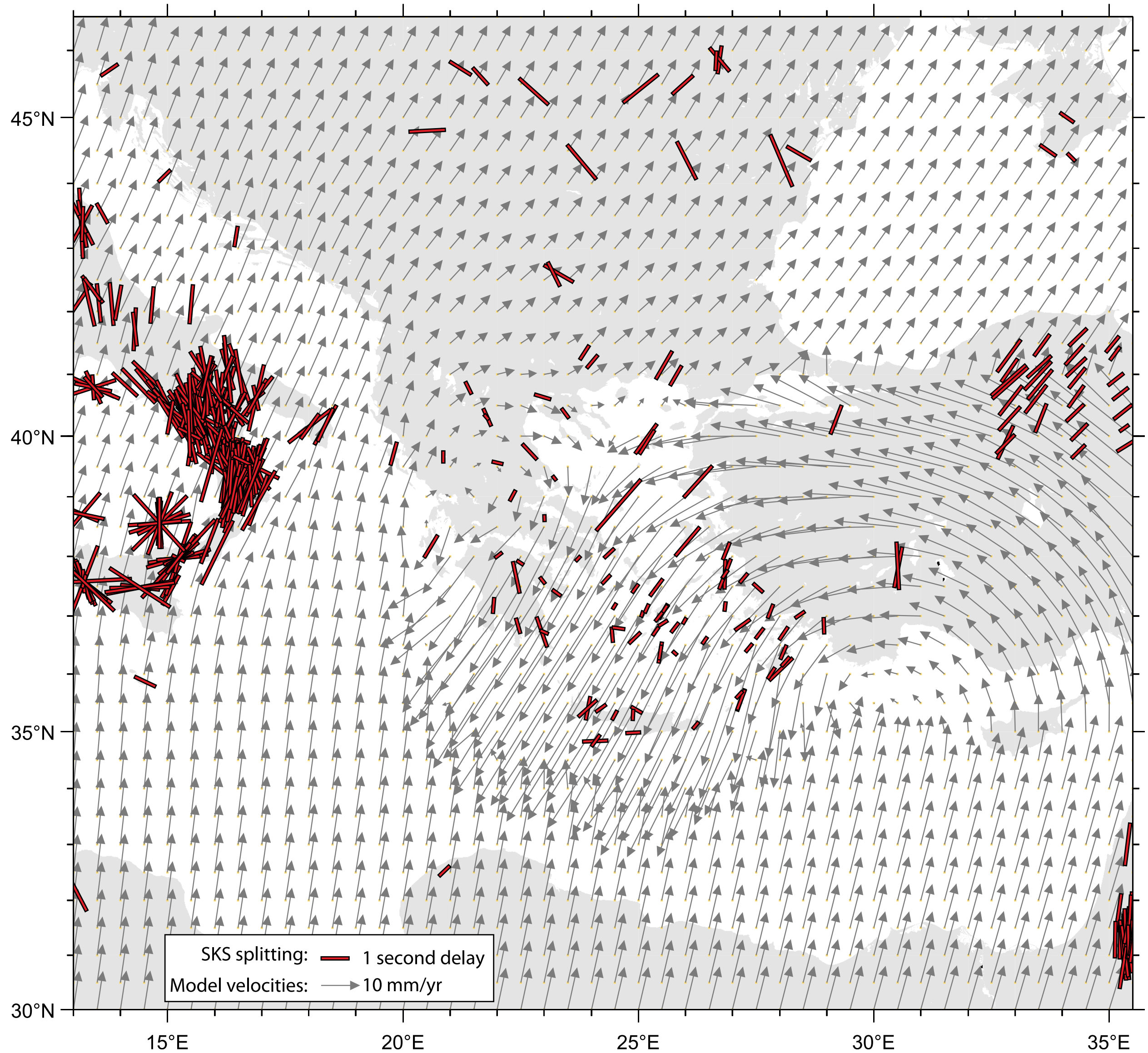


**Figure 12.** SKS splitting observations in Central and Eastern Mediterranean superimposed on our modeled Absolute Plate Motion. Shear wave splitting compilation is from *Wüstefeld et al.* [2009], database available online at http://www.gm.univ-montp2.fr/splitting/DB/.

difference is that extension is not restricted to the tip of a propagating fault, but spread over a wide region. The dynamic source for the extension is not the propagation of a throughgoing Anatolian Fault, but the regional retreat of the Hellenic slab.

### 5.2. Tectonic Boundaries and Kinematics of the Apulian-Ionian Block

[33] Figure 9 helps in visualizing groups of cells that have similar motion (i.e., Apulian-Ionian block and/or Nubia motion). The rotation pole of the Apulian-Ionian block relative to Nubia, located in the Sirte plain, nicely describes the opening of the Pelagian grabens (Figures 9 and 12). Our prediction for the opening of the Pelagian grabens is around 2–2.5 mm/ yr, similar to the results of *D'Agostino et al.* [2008]. *D'Agostino et al.* [2011a] also recently suggested that the western boundary of this ill-defined Apulian-Ionian block may follow the Malta scarp.

[34] Since the pole of rotation of the Apulian-Ionian block with respect to Nubia is in the Sirte Plain, little deformation is expected in this region. However, fragmentation of the deep Ionian Sea and its margins or reactivation of WNW-ESE Mesozoic faults

of the offshore continental shelf of Libya may well be responsible for the seismotectonics of Libya, frequently affected by earthquakes both offshore and onshore [*Westaway*, 1990; *Suleiman and Doser*, 1995; *Capitanio et al.*, 2011]. The tectonic regime inferred from the focal mechanisms in Libya is not conclusive. In any case, we propose that seismicity in Libya is related to the motion of the Apulian-Ionian block relative to Nubia.

[35] The small trenchward motion of the Calabria Arc with respect to the Apulian-Ionian block (~2–2.5 mm/yr) may correspond to a residual trench retreat [*D'Agostino et al.*, 2011a], Calabria being seen as one of the ultraslow subduction of the Mediterranean domain (together with Gibraltar [*Gutscher et al.*, 2006]). The alternative is that this motion is purely gravity driven and accommodated by large-scale collapse structures. Such structures are clearly seen within the Calabria wedge, in particular at the contact between the wedge and the backstop. We thus propose that the Calabria subduction is now inactive.

[36] Continental collision (or continental subduction?) between the Apulian-Ionian block and the Albania-western Greece is compatible with the ~5 mm/yr of shortening, purely frontal or with an oblique component (Figure 9). Jump of convergence rate from this ~5 mm/yr to ~26 mm/yr below Peloponnesus is accommodated by the dextral Kefalonia Fault and coincides with the transition from continental collision to oceanic subduction respectively [*Pearce et al.*, 2012]. The fault-parallel component increases SE away from the Kefalonia Fault (Figure 9). This remains complex to interpret as there might be a trade-off between distributed dextral strike-slip deformation [*Shaw and Jackson*, 2010], rigid clockwise rotation of upper plate blocks [*Cocard et al.*, 1999] and interseismic elastic loading [*Hollenstein et al.*, 2006] either on a vertical shear fault or on a more complex lateral ramp [*Govers and Wortel*, 2005; *Shaw and Jackson*, 2010; *Royden and Papanikolaou*, 2011]. As a result, the long-term slip rate of the Kefalonia Fault is difficult to assess and further studies would be required to better constrain the velocity field around the Ionian Islands. Our model suggests a long-term range of slip bracketed between 8 to 26 mm/yr (Figure 9).

## 5.3. Relationship Between Surface Plate Motions and Asthenospheric Flows

[37] In subduction zones affected by slab roll-back, toroïdal flows in the asthenosphere (flow transferring around a slab edge asthenosphere from the bottom side to the top side of the slab) is a well established concept validated by analogue [e.g., *Schellart*, 2004; *Funiciello et al.*, 2006] and numerical experiments [e.g., *Piromallo et al.*, 2006; *Stegman et al.*, 2006]. Deep asthenospheric toroïdal flows have been invoked in several subduction zones to account for the circular pattern of the fast-axis direction of SKS shear wave splitting around slab edges, such as in the Western U.S. [*Zandt and Humphreys*, 2008] or Calabria [*Civello and Margheriti*, 2004].

[38] A striking feature of our velocity field in the APM reference frame (Figure 10) is the occurrence of two apparent toroïdal patterns located above both ends of the Hellenic subduction zone. Crustal toroïdal motions may possibly be the surface expression of deep asthenospheric toroïdal flows around slab edges. Dynamic models of mantle flows based on tomographic data suggest significant contribution of mantle flows to account for surface motions in the Mediterranean [*Boschi et al.*, 2010; *Faccenna and Becker*, 2010]. Would this apply at both ends of the Hellenic subduction?

[39] *Le Pichon and Kreemer* [2010] propose a direct link between the surface toroïdal surface motion located around the eastern edge of the Hellenic subduction zone and flow of the mantle below. The Upper Miocene uplift and volcanism in the East Anatolian Plateau has been attributed to an asthenospheric rise [*Şengör et al.*, 2003] due to slab tear [*Govers and Wortel*, 2005; *Faccenna et al.*, 2006; *Keskin*, 2007] which is now well imaged by high resolution seismic tomography [*Paul et al.*, 2012]. The roll-back and the break-off of the Eastern Hellenic slab would enable the occurrence of an underlying asthenospheric toroïdal flow which would account for the circular counter-clockwise motion extending from the Levant to the Aegean in APM reference frame [*Le Pichon and Kreemer*, 2010]. Discussing the mantle flow issue at the NW end of the Hellenic subduction zone is more complex as the geometry of the Hellenic slab is still debated in this region. *Wortel and Spakman* [2000] propose an along-strike slab tear in the western Aegean to account for the increase of the arc curvature south of the Kefalonia Fault. Other studies propose a perpendicular slab tear below the Kefalonia transform [*Suckale et al.*, 2009; *Royden and Papanikolaou*, 2011].

[40] The simplest interpretation is toroïdal motions located at both ends of the Hellenic subduction zone (Figure 11) are reflecting the same mechanism, which could be slab tearing and subsequent toroïdal

mantle flow. Interestingly, proposing a symmetric mechanism at both end of the Hellenic subduction zone could explain the similarities in direction and in opening rate between the Gulf of Corinth and the western Turkey grabens. Nevertheless, a size dis-symmetry exists between the two toroïdal patterns, the radius being ~200 km in NW Greece versus ~500 km in Anatolia-Aegean. Our hypothesis is that the eastern flow started before the western one, triggering the large-scale rotation motion of the Anatolia-Aegean. Our results show that the western toroïdal pattern is centered in NW continental Greece, so that the slab tear would presently be located in the northern Aegean, as suggested by recent high-resolution tomography [*Paul et al.*, 2012], rather than below the Ionian islands [*Suckale et al.*, 2009; *Royden and Papanikolaou*, 2011].

## 5.4. Relationship Between Surface Plate Motions and Anisotropy

[41] Recent seismic anisotropy studies reveal that the NNE-SSW direction of fast-axis SKS previously measured in the Aegean domain [*Hatzfeld et al.*, 2001] actually spread over the entire Anatolian domain [*Wüstefeld et al.*, 2009; *Mutlu et al.*, 2010; *Paul et al.*, 2010]. The shear wave splitting database of *Wüstefeld et al.* [2009] is plotted in Figure 12. This result seems to invalidate previous interpretation of mantle flow in the Aegean exclusively linked to slab roll-back induced flows, following a model initially proposed by *Long and Silver* [2008]. Following this model, NW-SE directed SKS above Peloponnesus would represent trench parallel flow in the sub-slab domain, while NE-SW directed SKS in the Aegean domain – collinear with Miocene stretching lineations – would be due to the trench perpendicular corner flow in the mantle wedge of the overriding plate [*Jolivet et al.*, 2009; *Brun and Sokoutis*, 2010].

[42] The NE-SW oriented anisotropy measured over eastern and western Anatolia is more or less aligned with Eurasia or Nubia motion in an absolute frame. This could imply that the various blocks that form today Anatolia had a motion – backward or forward – more or less parallel to Nubia APM. Comparison of SKS splitting with absolute plate motions must however be considered with caution in the Eastern Mediterranean. SKS splitting most probably relates to global mantle circulation, but uncertainties remain at regional scale for areas with tectonics complexities, such as subduction systems [*Long and Becker*, 2010]. In any case, the anisotropy does not follow the Anatolia absolute plate motion, as already noticed by *Le Pichon and Kreemer* [2010], as if this motion had yet no imprint in the olivine Latticed Preferred Orientation (LPO) [*Kreemer et al.*, 2004]. The observed anisotropy may also be the result of several processes superimposed in time and space: the fast-axis directions may partly reflect frozen fossil olivine-LPO contained in the lithosphere as found in continental areas [*Silver*, 1996; *Fouch and Rondenay*, 2006], eventually superimposed onto a present-day flow or being the integration of a complex layered anisotropy [*Le Pichon and Kreemer*, 2010; *Lebedev et al.*, 2012].

[43] Our results show that the toroïdal surface motion observed in NW Greece is not associated with a rotation of the SKS fast axis direction, which are dominantly NNE-SSW and NW-SE directed (Figure 12). On the other hand, the transition from localized shear along the NAF to distributed extension in the Southern Balkans coincides with a drop in the delay split time and a 90° change in the orientation of the fast-axis (high splitting with a NNE-SSW direction east of Thessaloniki Peninsula versus low splitting with a NW-SE direction west of Thessaloniki Peninsula, Figure 12). This drop in anisotropy in northern Aegean coincides with the slab tear location proposed by *Paul et al.* [2012] inferred from high-resolution tomography. Occurrence of clockwise toroïdal pattern in APM at the same location is one more argument in favor of slab tearing.

## 5.5. When Was the Present-Day Strain Rate Field Established?

[44] An interesting but challenging point is to assess how far back in time can the present-day strain field be extrapolated. As mentioned in the introduction, a number of tectonic events still at work today actually started in the Late Miocene-Early Pliocene: earliest extension in the Corinth Gulf [*Collier and Dart*, 1991], switch of orientation of the normal faults in western Bulgaria – northern Greece from NW to purely E-W (ca. 3.6 Ma) [*Dinter and Royden*, 1993; *Burchfiel et al.*, 2008], E-W steep normal fault in western Turkey initiated in Pliocene times [*Yilmaz et al.*, 2000; *Bozkurt and Sozbilir*, 2004], dextral strike-slip activity on the North Anatolian Fault (NAF) in Northern Aegean in Early Pliocene times [*Armijo et al.*, 1999]. This tectonic regime was firmly established in Pleistocene time, with the acceleration and narrowing of the extension in the Gulf of Corinth [*Rohais et al.*, 2007], and the change from

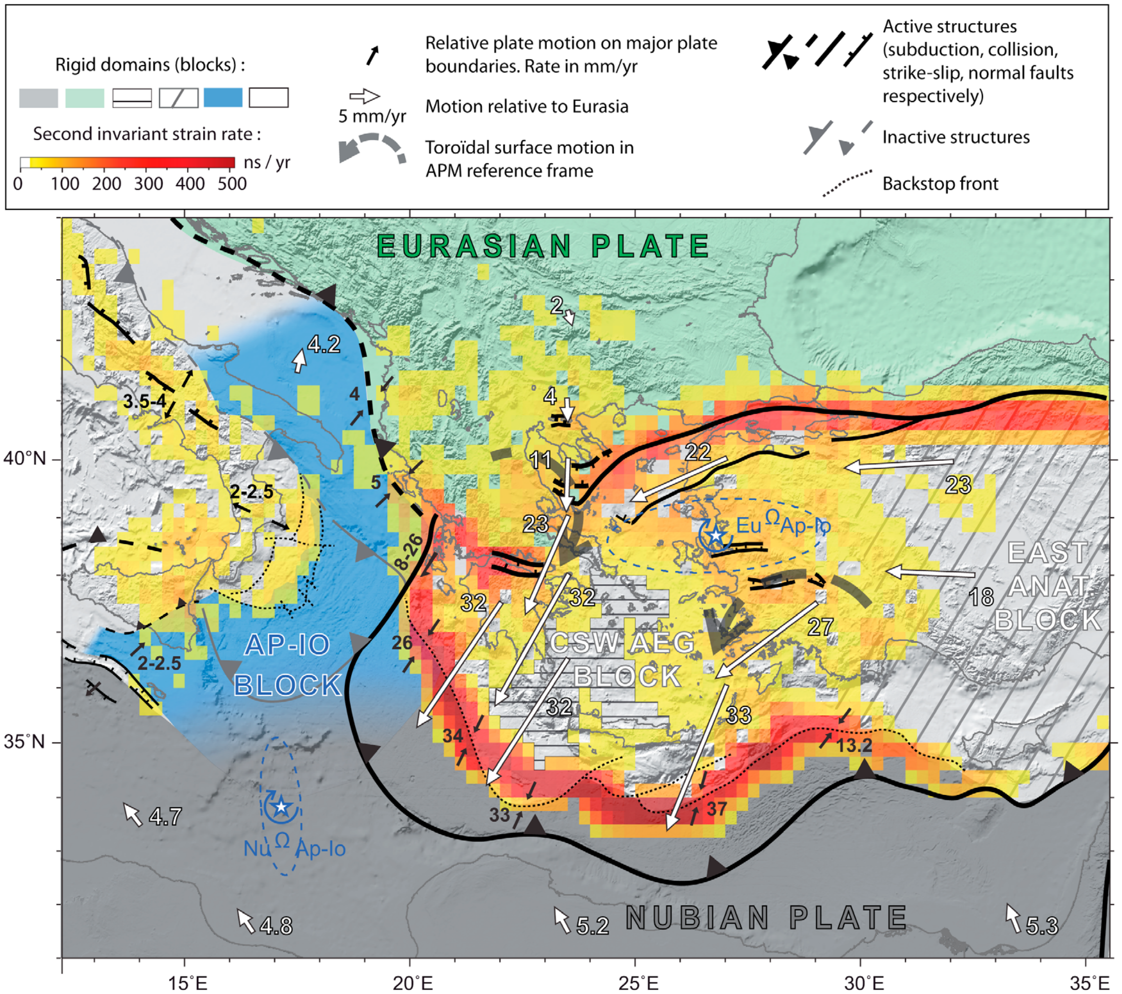


**Figure 13.** Present-day kinematic and tectonic map encompassing the Central and Eastern Mediterranean, summarizing our main results and interpretations. Our kinematic model includes rigid-block motions as well as localized and distributed strain. Central-SW Aegean block (CSW AEG block) and East Anatolian block (East Anat. block) are purely kinematic and directly results from strain modeling (Figure 5). AP-IO Block is our Apulian-Ionian block with tentative tectonic boundaries. Rotation pole of this Apulian-Ionian block relative to Nubia (Nu $^{\Omega}$Ap-Io) and to Eurasia (Eu $^{\Omega}$Ap-Io) are shown with their 95% confidence ellipse.

transpression to transtension along the western portion of the NAF [*Bellier et al.*, 1997].

[45] According to many studies, the westward propagation of the NAF in the Aegean in Pliocene times is the dynamic source that triggered the opening of E-W trending gulfs in western Aegean [*Armijo et al.*, 1996; *Goldsworthy et al.*, 2002; *Flerit et al.*, 2004; *Reilinger et al.*, 2010; *Shaw and Jackson*, 2010].

[46] The timing of the events affecting the Eastern Mediterranean since Late Miocene is compatible with an alternative scenario: A single recent stage of slab retreat, initiated in the Late Miocene-Early Pliocene and still active today, caused N-S rifting in the Gulf of Corinth and in western Anatolia and turned extension in Southern Balkans to purely N-S directed. The NAF, accommodating Eurasia/Anatolia relative motion, reached the Aegean in Pliocene times. However, the NAF did not propagate westward of the Thessaloniki peninsula as the relative motion between stable Eurasia and the south Aegean was gradually accommodated by widespread N-S extension from the Southern Balkans to the eastern Gulf of Corinth. This scenario is in agreement with studies that propose rifting in the Gulf of Corinth to be due to basal shear and gravitational collapse associated to the retreat of the Hellenic slab [*Jolivet*, 2001; *Le Pourhiet et al.*, 2003; *Jolivet et al.*, 2008, 2010].

[47] Quaternary temporal markers are less abundant in the Central Mediterranean (Sirte, Libya and the Pelagian rifts). We propose that the present-day strain field settled during the Plio-Quaternary, after the slow-down of slab retreat of the Calabrian slab and the last episode of back-arc extension in the Tyrrhenian Basin in the late Pliocene. This is in agreement with the Plio-Pleistocene reactivation of the NW-SE extensive structures of the Pelagian rift [*Torelli et al.*, 1995] and the Holocene activity of normal faults in the Apennines [*Palumbo et al.*, 2004].

## 6. Conclusions

[48] We performed kinematic and strain modeling of an area that encompasses Central Mediterranean and Eastern Mediterranean, applying *Haines and Holt*'s [1993] method to derive a continuous velocity field compatible with GPS velocities and focal mechanisms. As it is large-scale, our model allows connecting the kinematics of regions that have often been studied independently: Calabrian subduction zone, Ionian Basin, Hellenic subduction zone, western Greece, Balkans, Aegean domain, Anatolia. The main results are the following:

[49] (1) The Southern Balkans (Western Bulgaria, Macedonia) and continental Greece do not belong to stable Eurasia and are moving southward with respect to Eurasia. We show that the distributed N-S directed extension occurring in the Thessaloniki Peninsula [*Burchfiel et al.*, 2006; *Kotzev et al.*, 2006] is actually spreading and increasing further south, and reaches the eastern Gulf of Corinth. Relative motion between stable Eurasia and the Aegean domain in the western Aegean is thus gradually accommodated by distributed extension, so that the westward propagation of the NAF throughout continental Greece or Peloponnesus is not required (i.e., extension in Southern Balkans deactivates the western tip of the NAF). Consequently, termination of the dextral NAF would be located south of the Thessaloniki Peninsula, where the NAF fault system turns into spoon-shaped E-W normal faults (Figure 11c).

[50] The southward (and trenchward) motion of the entire Southern Balkans-continental Greece follows a flow-like pattern. This pattern, clearly toroïdal in the APM reference frame, mimics a deeper flow located either in the ductile lower crust or deeper in the asthenosphere, probably associated with the retreating Hellenic slab.

[51] (2) We further constrain the fragmentation of the oceanic Ionian lithosphere offshore. Following *D'Agostino et al.* [2008], we show that a single rigid rotation can minimize the motion of the Hyblean Plateau, the Apulia Peninsula, the south Adriatic Sea, the Ionian Basin and the Sirte plain. This Apulian-Ionian block (Figures 9 and 13) has a clockwise motion relative to Nubia around a pole located in the Sirte Plain. Relative motion of this Apulian-Ionian block with respect to the Nubian plate explains the seismotectonics of Libya and the opening of the Pelagian rifts (2–2.5 mm/yr). The Apulian-Ionian block collides against the Eurasian plate along the Albania-Western Greece coast ($\sim$5 mm/yr of shortening). Our results emphasize the contrasting velocities of trenchward motion affecting the subducting Nubian plate: ultraslow in the Calabrian subduction zone (2–2.5 mm/yr) and fast in the Hellenic subduction zone ($\sim$30 mm/yr). It suggests that the Calabrian subduction zone is now inactive, so that ultraslow trenchward motion of Calabria can be considered as pure gravitational collapse rather than trench retreat. On the contrary, fast trench retreat is consuming the Ionian lithosphere along the Hellenic subduction zone.

[52] (3) Finally, the modeled velocity field in the Absolute Plate Motion reference frame depicts two crustal toroïdal patterns located at both ends of the Hellenic subduction zone. These crustal toroïdal motions are respectively clockwise at the NW end of the Hellenic subduction zone and counterclockwise at its eastern end (Figure 10). The simplest solution is that both toroïdal flows are related to slab tears, the Hellenic slab now being detached from its two buoyant pieces of continental lithosphere on either sides, respectively the Apulian platform to the west and continental fragments off Anatolia to the east.

## Acknowledgments

[53] We are grateful to the Editor T. Becker, N. D'Agostino and an anonymous reviewer and for their constructive reviews and suggestions which led to considerable improvements in our manuscript. We also thank A. Paul and L. Jolivet for fruitful discussions and for having shown us pre-print or not yet published materials. This research has benefited from funding provided by the Laboratoire Yves-Rocard (LRC).

## References

Aktug, B., et al. (2009), Deformation of western Turkey from a combination of permanent and campaign GPS data: Limits to block-like behavior, *J. Geophys. Res.*, *114*, B10404, doi:10.1029/2008JB006000.

Alvarez, W. (1990), Geologic evidence for the plate-driving mechanism: The continental undertow hypothesis and the Australian-Antarctic Discordance, *Tectonics*, *9*(5), 1213–1220, doi:10.1029/TC009i005p01213.

Alvarez, W. (2010), Protracted continental collisions argue for continental plates driven by basal traction, *Earth Planet. Sci. Lett.*, *296*(3–4), 434–442, doi:10.1016/j.epsl.2010.05.030.

Argus, D. F., R. G. Gordon, M. B. Heflin, C. Ma, R. J. Eanes, P. Willis, W. R. Peltier, and S. E. Owen (2010), The angular velocities of the plates and the velocity of Earth's centre from space geodesy, *Geophys. J. Int.*, *180*(3), 913–960, doi:10.1111/j.1365-246X.2009.04463.x.

Armijo, R., B. Meyer, G. C. P. King, A. Rigo, and D. Papanastassiou (1996), Quaternary evolution of the Corinth Rift and its implications for the Late Cenozoic evolution of the Aegean, *Geophys. J. Int.*, *126*(1), 11–53, doi:10.1111/j.1365-246X.1996.tb05264.x.

Armijo, R., B. Meyer, A. Hubert, and A. Barka (1999), Westward propagation of the North Anatolian Fault into the northern Aegean: Timing and kinematics, *Geology*, *27*(3), 267–270, doi:10.1130/0091-7613(1999)027<0267:WPOTNA>2.3.CO;2.

Beaumont, C., R. A. Jamieson, M. H. Nguyen, and S. Medvedev (2004), Crustal channel flows: 1. Numerical models with applications to the tectonics of the Himalayan-Tibetan orogen, *J. Geophys. Res.*, *109*, B06406, doi:10.1029/2003JB002809.

Beavan, J., and J. Haines (2001), Contemporary horizontal velocity and strain rate fields of the Pacific-Australian plate boundary zone through New Zealand, *J. Geophys. Res.*, *106*(B1), 741–770, doi:10.1029/2000JB900302.

Becker, T. W. (2008), Azimuthal seismic anisotropy constrains net rotation of the lithosphere, *Geophys. Res. Lett.*, *35*, L05303, doi:10.1029/2007GL032928.

Bellier, O., S. Over, A. Poisson, and J. Andrieux (1997), Recent temporal change in the stress state and modern stress field along the North Anatolian Fault Zone (Turkey), *Geophys. J. Int.*, *131*(1), 61–86, doi:10.1111/j.1365-246X.1997.tb00595.x.

Benedetti, L. (1999), Sismotectonique de l'Italie et des régions adjacentes: Fragmentation du promontoire adriatique, PhD thesis, 358 pp., Univ. Paris VII, Paris.

Bennett, R. A., S. Hreinsdottir, G. Buble, T. Basic, Z. Bacic, M. Marjanovic, G. Casale, A. Gendaszek, and D. Cowan (2008), Eocene to present subduction of southern Adria mantle lithosphere beneath the Dinarides, *Geology*, *36*(1), 3–6, doi:10.1130/G24136A.1.

Bokelmann, G. H. R. (2002), Which forces drive North America?, *Geology*, *30*(11), 1027–1030, doi:10.1130/0091-7613(2002)030<1027:WFDNA>2.0.CO;2.

Boschi, L., C. Faccenna, and T. W. Becker (2010), Mantle structure and dynamic topography in the Mediterranean Basin, *Geophys. Res. Lett.*, *37*, L20303, doi:10.1029/2010GL045001.

Bozkurt, E., and H. Sozbilir (2004), Tectonic evolution of the Gediz Graben: Field evidence for an episodic, two-stage extension in western Turkey, *Geol. Mag.*, *141*(1), 63–79, doi:10.1017/S0016756803008379.

Briole, P., A. Rigo, H. Lyon-Caen, J. C. Ruegg, K. Papazissi, C. Mitsakaki, A. Balodimou, G. Veis, D. Hatzfeld, and A. Deschamps (2000), Active deformation of the Corinth rift, Greece: Results from repeated Global Positioning System surveys between 1990 and 1995, *J. Geophys. Res.*, *105*(B11), 25,605–25,625, doi:10.1029/2000JB900148.

Brun, J. P., and C. Faccenna (2008), Exhumation of high-pressure rocks driven by slab rollback, *Earth Planet. Sci. Lett.*, *272*(1–2), 1–7, doi:10.1016/j.epsl.2008.02.038.

Brun, J. P., and D. Sokoutis (2010), 45 m.y. of Aegean crust and mantle flow driven by trench retreat, *Geology*, *38*(9), 815–818, doi:10.1130/G30950.1.

Burchfiel, B. C., R. Nakov, T. Tzankov, and L. H. Royden (2000), Cenozoic extension in Bulgaria and northern Greece: The northern part of the Aegean extensional regime, in *Tectonics and Magmatism in Turkey and the Surrounding Area*, edited by E. Bozkurt, J. A. Winchester, and J. D. A. Piper, *Geol. Soc. Spec. Publ.*, 173, 325–352, doi:10.1144/GSL.SP.2000.173.01.16.

Burchfiel, B. C., R. W. King, A. Todosov, V. Kotzev, N. Durmurdzanov, T. Serafimovski, and B. Nurce (2006), GPS results for Macedonia and its importance for the tectonics of the Southern Balkan extensional regime, *Tectonophysics*, *413*(3–4), 239–248, doi:10.1016/j.tecto.2005.10.046.

Burchfiel, B. C., R. Nakov, N. Dumurdzanov, D. Papanikolaou, T. Tzankov, T. Serafimovski, R. W. King, V. Kotzev, A. Todosov, and B. Nurce (2008), Evolution and dynamics of the Cenozoic tectonics of the South Balkan extensional system, *Geosphere*, *4*(6), 919–938, doi:10.1130/GES00169.1.

Calais, E., C. DeMets, and J. M. Nocquet (2003), Evidence for a post-3.16-Ma change in Nubia Eurasia North America plate motions?, *Earth Planet. Sci. Lett.*, *216*(1–2), 81–92, doi:10.1016/S0012-821X(03)00482-5.

Capitanio, F. A., C. Faccenna, R. Funiciello, and F. Salvini (2011), Recent tectonics of Tripolitania, Libya: An intraplate record of Mediterranean subduction, *Geol. Soc. Spec. Publ.*, *357*, 319–328, doi:10.1144/SP357.17.

Chamot-Rooke, N., C. Rangin, X. Le Pichon, and Dotmed Working Group (2005), DOTMED: A synthesis of deep marine data in the eastern Mediterranean, *Mem. Soc. Geol. Fr.*, *177*(64), 64 pp.

Channell, J. E. T. (1996), Palaeomagnetism and palaeogeography of Adria, in *Palaeomagnetism and Tectonics of the Mediterranean Region*, edited by A. Morris and D. H. Tarling, *Geol. Soc. Spec. Publ.*, 105, 119–132.

Charara, R. (2010), GPS statique, cinématique et haute fréquence appliqué à l'étude de déformations de zones sismiques, PhD thesis, 103 pp., Lab. de Géol., l'Ecole Normale Supérieure, Paris.

Civello, S., and L. Margheriti (2004), Toroidal mantle flow around the Calabrian slab (Italy) from SKS splitting, *Geophys. Res. Lett.*, *31*, L10601, doi:10.1029/2004GL019607.

Cocard, M., H. G. Kahle, Y. Peter, A. Geiger, G. Veis, S. Felekis, D. Paradissis, and H. Billiris (1999), New constraints on the rapid crustal motion of the Aegean region: Recent results inferred from GPS measurements (1993–1998) across the West Hellenic Arc, Greece, *Earth Planet. Sci. Lett.*, *172*(1–2), 39–47, doi:10.1016/S0012-821X(99)00185-5.

Collier, R. E. L., and C. J. Dart (1991), Neogene to Quaternary rifting, sedimentation and uplift in the Corinth Basin, Greece, *J. Geol. Soc.*, *148*, 1049–1065, doi:10.1144/gsjgs.148.6.1049.

D'Agostino, N., A. Avallone, D. Cheloni, E. D'Anastasio, S. Mantenuto, and G. Selvaggi (2008), Active tectonics of the Adriatic region from GPS and earthquake slip vectors, *J. Geophys. Res.*, *113*, B12413, doi:10.1029/2008JB005860.

D'Agostino, N., E. D'Anastasio, A. Gervasi, I. Guerra, M. R. Nedimovic, L. Seeber, and M. Steckler (2011a), Forearc extension and slow rollback of the Calabrian Arc from GPS measurements, *Geophys. Res. Lett.*, *38*, L17304, doi:10.1029/2011GL048270.

D'Agostino, N., S. Mantenuto, E. D'Anastasio, R. Giuliani, M. Mattone, S. Calcaterra, P. Gambino, and L. Bonci (2011b), Evidence for localized active extension in the central Apennines (Italy) from global positioning system observations, *Geology*, *39*(4), 291–294, doi:10.1130/G31796.1.

Devoti, R., A. Esposito, G. Pietrantonio, A. R. Pisani, and F. Riguzzi (2011), Evidence of large scale deformation patterns from GPS data in the Italian subduction boundary, *Earth Planet. Sci. Lett.*, *311*(3–4), 230–241, doi:10.1016/j.epsl.2011.09.034.

Dewey, J. F., M. L. Helman, E. Torco, D. H. W. Hutton, and S. D. Knott (1989), Kinematics of the western Mediterranean, in *Alpine Tectonics*, edited by M. P. Coward, D. D. Dietrich, and R. G. Park, *Geol. Soc. Spec. Publ.*, 45, 265–283.

Dinter, D. A., and L. Royden (1993), Late Cenozoic extension in northeastern Greece: Strymon Valley detachment system and Rhodope metamorphic core complex, *Geology*, *21*(1), 45–48, doi:10.1130/0091-7613(1993)021<0045:LCEING>2.3.CO;2.

Engdahl, E. R., R. van der Hilst, and R. Buland (1998), Global teleseismic earthquake relocation with improved travel times and procedures for depth determination, *Bull. Seismol. Soc. Am.*, *88*(3), 722–743.

Faccenna, C., and T. W. Becker (2010), Shaping mobile belts by small-scale convection, *Nature*, *465*(7298), 602–605, doi:10.1038/nature09064.

Faccenna, C., T. W. Becker, F. P. Lucente, L. Jolivet, and F. Rossetti (2001), History of subduction and back-arc extension in the central Mediterranean, *Geophys. J. Int.*, *145*(3), 809–820, doi:10.1046/j.0956-540x.2001.01435.x.

Faccenna, C., C. Piromallo, A. Crespo-Blanc, L. Jolivet, and F. Rossetti (2004), Lateral slab deformation and the origin of the western Mediterranean arcs, *Tectonics*, *23*, TC1012, doi:10.1029/2002TC001488.

Faccenna, C., O. Bellier, J. Martinod, C. Piromallo, and V. Regard (2006), Slab detachment beneath eastern Anatolia: A possible cause for the formation of the North Anatolian Fault, *Earth Planet. Sci. Lett.*, *242*(1–2), 85–97, doi:10.1016/j.epsl.2005.11.046.

Flerit, F., R. Armijo, G. King, and B. Meyer (2004), The mechanical interaction between the propagating North Anatolian Fault and the back-arc extension in the Aegean, *Earth Planet. Sci. Lett.*, *224*(3–4), 347–362, doi:10.1016/j.epsl.2004.05.028.

Floyd, M. A., et al. (2010), A new velocity field for Greece: Implications for the kinematics and dynamics of the Aegean, *J. Geophys. Res.*, *115*, B10403, doi:10.1029/2009JB007040.

Fouch, M. J., and S. Rondenay (2006), Seismic anisotropy beneath stable continental interiors, *Phys. Earth Planet. Inter.*, *158*(2–4), 292–320, doi:10.1016/j.pepi.2006.03.024.

Funiciello, F., M. Moroni, C. Piromallo, C. Faccenna, A. Cenedese, and H. A. Bui (2006), Mapping mantle flow during retreating subduction: Laboratory models analyzed by feature tracking, *J. Geophys. Res.*, *111*, B03402, doi:10.1029/2005JB003792.

Gautier, P., J. P. Brun, R. Moriceau, D. Sokoutis, J. Martinod, and L. Jolivet (1999), Timing, kinematics and cause of Aegean extension: A scenario based on a comparison with simple analogue experiments, *Tectonophysics*, *315*(1–4), 31–72, doi:10.1016/S0040-1951(99)00281-4.

Goldsworthy, M., J. Jackson, and J. Haines (2002), The continuity of active fault systems in Greece, *Geophys. J. Int.*, *148*(3), 596–618, doi:10.1046/j.1365-246X.2002.01609.x.

Govers, R., and M. J. R. Wortel (2005), Lithosphere tearing at STEP faults: Response to edges of subduction zones, *Earth Planet. Sci. Lett.*, *236*(1–2), 505–523, doi:10.1016/j.epsl.2005.03.022.

Gripp, A. E., and R. G. Gordon (2002), Young tracks of hotspots and current plate velocities, *Geophys. J. Int.*, *150*(2), 321–361, doi:10.1046/j.1365-246X.2002.01627.x.

Gutscher, M. A., J. Roger, M. A. Baptista, J. M. Miranda, and S. Tinti (2006), Source of the 1693 Catania earthquake and tsunami (southern Italy): New evidence from tsunami modeling of a locked subduction fault plane, *Geophys. Res. Lett.*, *33*, L08309, doi:10.1029/2005GL025442.

Haines, A. J., and W. E. Holt (1993), A procedure for obtaining the complete horizontal motions within zones of distributed deformation from the inversion of strain-rate data, *J. Geophys. Res.*, *98*(B7), 12,057–12,082, doi:10.1029/93JB00892.

Hatzfeld, D., E. Karagianni, I. Kassaras, A. Kiratzi, E. Louvari, H. Lyon-Caen, K. Makropoulos, P. Papadimitriou, G. Bock, and K. Priestley (2001), Shear wave anisotropy in the upper mantle beneath the Aegean related to internal deformation, *J. Geophys. Res.*, *106*(B12), 30,737–30,753, doi:10.1029/2001JB000387.

Hoink, T., A. M. Jellinek, and A. Lenardic (2011), Viscous coupling at the lithosphere-asthenosphere boundary, *Geochem. Geophys. Geosyst.*, *12*, Q0AK02, doi:10.1029/2011GC003698.

Hollenstein, C., A. Geiger, H. G. Kahle, and G. Veis (2006), CGPS time-series and trajectories of crustal motion along the West Hellenic Arc, *Geophys. J. Int.*, *164*(1), 182–191, doi:10.1111/j.1365-246X.2005.02804.x.

Hollenstein, C., M. D. Muller, A. Geiger, and H. G. Kahle (2008), Crustal motion and deformation in Greece from a decade of GPS measurements, 1993–2003, *Tectonophysics*, *449*(1–4), 17–40, doi:10.1016/j.tecto.2007.12.006.

Jolivet, L. (2001), A comparison of geodetic and finite strain pattern in the Aegean, geodynamic implications, *Earth Planet. Sci. Lett.*, *187*(1–2), 95–104, doi:10.1016/S0012-821X(01)00277-1.

Jolivet, L., and J. P. Brun (2010), Cenozoic geodynamic evolution of the Aegean, *Int. J. Earth Sci.*, *99*(1), 109–138, doi:10.1007/s00531-008-0366-4.

Jolivet, L., R. Augier, C. Faccenna, F. Negro, G. Rimmele, P. Agard, C. Robin, F. Rossetti, and A. Crespo-Blanc (2008), Subduction, convergence and the mode of backarc extension in the Mediterranean region, *Bull. Soc. Geol. Fr.*, *179*(6), 525–550, doi:10.2113/gssgfbull.179.6.525.

Jolivet, L., C. Faccenna, and C. Piromallo (2009), From mantle to crust: Stretching the Mediterranean, *Earth Planet. Sci. Lett.*, *285*(1–2), 198–209, doi:10.1016/j.epsl.2009.06.017.

Jolivet, L., L. Labrousse, P. Agard, O. Lacombe, V. Bailly, E. Lecomte, F. Mouthereau, and C. Mehl (2010), Rifting and shallow-dipping detachments, clues from the Corinth Rift and the Aegean, *Tectonophysics*, *483*(3–4), 287–304, doi:10.1016/j.tecto.2009.11.001.

Jouanne, F., J. L. Mugnier, R. Koci, S. Bushati, K. Matev, N. Kuka, I. Shinko, S. Kociu, and L. Duni (2012), GPS constrains on current tectonics of Albania, *Tectonophysics*, *554–557*, 50–62, doi:10.1016/j.tecto.2012.06.008.

Kahle, H. G., R. Cocard, Y. Peter, A. Geiger, R. Reilinger, S. McClusky, R. King, A. Barka, and G. Veis (1999), The GPS strain rate field in the Aegean Sea and western Anatolia, *Geophys. Res. Lett.*, *26*(16), 2513–2516, doi:10.1029/1999GL900403.

Keskin, M. (2007), Eastern Anatolia: A hotspot in a collision zone without a mantle plume, in *Plates, Plumes, and Planetary Processes*, edited by G. R. Foulger and D. M. Jurdy, *Spec. Pap. Geol. Soc. Am.*, 430, 693–722, doi:10.1130/2007.2430(32).

Kotzev, V., R. Nakov, T. Georgiev, B. C. Burchfiel, and R. W. King (2006), Crustal motion and strain accumulation in western Bulgaria, *Tectonophysics*, *413*(3–4), 127–145, doi:10.1016/j.tecto.2005.10.040.

Kreemer, C. (2009), Absolute plate motions constrained by shear wave splitting orientations with implications for hot spot motions and mantle flow, *J. Geophys. Res.*, *114*, B10405, doi:10.1029/2009JB006416.

Kreemer, C., and N. Chamot-Rooke (2004), Contemporary kinematics of the southern Aegean and the Mediterranean Ridge, *Geophys. J. Int.*, *157*(3), 1377–1392, doi:10.1111/j.1365-246X.2004.02270.x.

Kreemer, C., W. E. Holt, and A. J. Haines (2003), An integrated global model of present-day plate motions and plate boundary deformation, *Geophys. J. Int.*, *154*(1), 8–34, doi:10.1046/j.1365-246X.2003.01917.x.

Kreemer, C., N. Chamot-Rooke, and X. Le Pichon (2004), Constraints on the evolution and vertical coherency of deformation in the northern Aegean from a comparison of geodetic, geologic and seismologic data, *Earth Planet. Sci. Lett.*, *225*(3–4), 329–346, doi:10.1016/j.epsl.2004.06.018.

Lebedev, S., E. Neenan, B. Knapmeyer-Endrun, T. Meier, M. R. Agius, A. J. Schaeffer, C. Tirel, and W. Friederich (2012), Lithospheric dynamics in eastern Mediterranean: Insights from seismic structure and anisotropy, *Geophys. Res. Abstr.*, *14*, EGU2012-6626-2012.

Le Pichon, X., and C. Kreemer (2010), The Miocene-to-present kinematic evolution of the eastern Mediterranean and Middle East and its implications for dynamics, *Annu. Rev. Earth Planet. Sci.*, *38*(1), 323–351, doi:10.1146/annurev-earth-040809-152419.

Le Pichon, X., N. Chamot-Rooke, S. Lallemant, R. Noomen, and G. Veis (1995), Geodetic determination of the kinematics of central Greece with respect to Europe: Implications for eastern Mediterranean tectonics, *J. Geophys. Res.*, *100*(B7), 12,675–12,690.

Le Pourhiet, L., E. Burov, and I. Moretti (2003), Initial crustal thickness geometry controls on the extension in a back arc domain: Case of the Gulf of Corinth, *Tectonics*, *22*(4), 1032, doi:10.1029/2002TC001433.

Long, M. D., and T. W. Becker (2010), Mantle dynamics and seismic anisotropy, *Earth Planet. Sci. Lett.*, *297*(3–4), 341–354, doi:10.1016/j.epsl.2010.06.036.

Long, M. D., and P. G. Silver (2008), The subduction zone flow field from seismic anisotropy: A global view, *Science*, *319*(5861), 315–318, doi:10.1126/science.1150809.

Louvari, E., A. A. Kiratzi, and B. C. Papazachos (1999), The Cephalonia Transform Fault and its extension to western Lefkada Island (Greece), *Tectonophysics*, *308*(1–2), 223–236, doi:10.1016/S0040-1951(99)00078-5.

Malinverno, A., and W. B. F. Ryan (1986), Extension in the Tyrrhenian Sea and shortening in the Apennines as result of arc migration driven by sinking of the lithosphere, *Tectonics*, *5*(2), 227–245, doi:10.1029/TC005i002p00227.

McClusky, S., et al. (2000), Global Positioning System constraints on plate kinematics and dynamics in the eastern Mediterranean and Caucasus, *J. Geophys. Res.*, *105*(B3), 5695–5719.

Meyer, B., M. Sebrier, and D. Dimitrov (2007), Rare destructive earthquakes in Europe: The 1904 Bulgaria event case, *Earth Planet. Sci. Lett.*, *253*(3–4), 485–496, doi:10.1016/j.epsl.2006.11.011.

Mutlu, A. K., H. Karabulut, and A. Paul (2010), Seismic anisotropy and upper mantle velocity structure beneath Turkey and surrounding regions from Pn and SKS measurements, paper presented at 32nd General Assembly, Eur. Seismol. Comm., Montpellier, France.

Nyst, M., and W. Thatcher (2004), New constraints on the active tectonic deformation of the Aegean, *J. Geophys. Res.*, *109*, B11406, doi:10.1029/2003JB002830.

Özeren, M. S., and W. E. Holt (2010), The dynamics of the eastern Mediterranean and eastern Turkey, *Geophys. J. Int.*, *183*(3), 1165–1184, doi:10.1111/j.1365-246X.2010.04819.x.

Palumbo, L., L. Benedetti, D. Bourles, A. Cinque, and R. Finkel (2004), Slip history of the Magnola fault (Apennines, central Italy) from $Cl^{-}36$ surface exposure dating: Evidence for strong earthquakes over the Holocene, *Earth Planet. Sci. Lett.*, *225*(1–2), 163–176, doi:10.1016/j.epsl.2004.06.012.

Papanikolaou, D., M. Alexandri, and P. Nomikou (2006), Active faulting in the north Aegean basin, in *Postcollisional Tectonics and Magmatism in the Mediterranean Region and Asia*, *Spec. Pap. Geol. Soc. Am.*, *409*, 189–209, doi:10.1130/2006.2409(11).

Papazachos, B. C. (2002), The active crustal deformation field of the Aegean area inferred from seismicity and GPS data, paper presented at 11th General Assembly, WEGENER Proj., Athens.

Paul, A., W. Ben Mansour, D. Hatzfeld, H. Karabulut, D. M. Childs, C. Péquegnat, P. Hatzidimitriou, and the Simbaad Team (2010), Mantle flow in the Aegean-Anatolia region by SKS splitting measurements, *Geophys. Res. Abstr.*, *12*, EGU2010-8807-2011.

Paul, A., G. Salaün, H. Karabulut, H. A. Pedersen, and A. Kömec Mutlu (2012), Traces of subduction and their relation to seismic anisotropy beneath Greece and Turkey: New evidences and questions from seismic tomography, *Geophys. Res. Abstr.*, *14*, EGU2012-2913.

Pearce, F. D., S. Rondenay, M. Sachpazi, M. Charalampakis, and L. H. Royden (2012), Seismic investigation of the transition from continental to oceanic subduction along the western Hellenic Subduction Zone, *J. Geophys. Res.*, *117*, B07306, doi:10.1029/2011JB009023.

Piromallo, C., T. W. Becker, F. Funiciello, and C. Faccenna (2006), Three-dimensional instantaneous mantle flow induced by subduction, *Geophys. Res. Lett.*, *33*, L08304, doi:10.1029/2005GL025390.

Reilinger, R., et al. (2006), GPS constraints on continental deformation in the Africa-Arabia-Eurasia continental collision zone and implications for the dynamics of plate interactions, *J. Geophys. Res.*, *111*, B05411, doi:10.1029/2005JB004051.

Reilinger, R., S. McClusky, D. Paradissis, S. Ergintav, and P. Vernant (2010), Geodetic constraints on the tectonic evolution of the Aegean region and strain accumulation along the Hellenic subduction zone, *Tectonophysics*, *488*(1–4), 22–30, doi:10.1016/j.tecto.2009.05.027.

Rohais, S., R. Eschard, M. Ford, F. Guillocheau, and I. Moretti (2007), Stratigraphic architecture of the Plio-Pleistocene infill of the Corinth Rift: Implications for its structural evolution, *Tectonophysics*, *440*(1–4), 5–28, doi:10.1016/j.tecto.2006.11.006.

Rosenbaum, G., G. S. Lister, and C. Duboz (2004), The Mesozoic and Cenozoic motion of Adria (central Mediterranean): A review of constraints and limitations, *Geodin. Acta*, *17*(2), 125–139, doi:10.3166/ga.17.125-139.

Royden, L. H., and D. J. Papanikolaou (2011), Slab segmentation and late Cenozoic disruption of the Hellenic arc, *Geochem. Geophys. Geosyst.*, *12*, Q03010, doi:10.1029/2010GC003280.

Schellart, W. P. (2004), Kinematics of subduction and subduction-induced flow in the upper mantle, *J. Geophys. Res.*, *109*, B07401, doi:10.1029/2004JB002970.

Şengör, A. M. C., S. Ozeren, T. Genc, and E. Zor (2003), East Anatolian high plateau as a mantle-supported, north–south shortened domal structure, *Geophys. Res. Lett.*, *30*(24), 8045, doi:10.1029/2003GL017858.

Şengör, A. M. C., O. Tuysuz, C. Imren, M. Sakinc, H. Eyidogan, G. Gorur, X. Le Pichon, and C. Rangin (2005), The North Anatolian Fault: A new look, *Annu. Rev. Earth Planet. Sci.*, *33*, 37–112, doi:10.1146/annurev.earth.32.101802.120415.

Serpelloni, E., M. Anzidei, P. Baldi, G. Casula, and A. Galvani (2005), Crustal velocity and strain-rate fields in Italy and surrounding regions: New results from the analysis of permanent and non-permanent GPS networks, *Geophys. J. Int.*, *161*(3), 861–880, doi:10.1111/j.1365-246X.2005.02618.x.

Shaw, B., and J. Jackson (2010), Earthquake mechanisms and active tectonics of the Hellenic subduction zone, *Geophys. J. Int.*, *181*(2), 966–984.

Silver, P. G. (1996), Seismic anisotropy beneath the continents: Probing the depths of geology, *Annu. Rev. Earth Planet. Sci.*, *24*, 385, doi:10.1146/annurev.earth.24.1.385.

Stampfli, G. M., and G. D. Borel (2002), A plate tectonic model for the Paleozoic and Mesozoic constrained by dynamic plate boundaries and restored synthetic oceanic isochrons, *Earth Planet. Sci. Lett.*, *196*(1–2), 17–33, doi:10.1016/S0012-821X(01)00588-X.

Stegman, D. R., J. Freeman, W. P. Schellart, L. Moresi, and D. May (2006), Influence of trench width on subduction hinge retreat rates in 3-D models of slab rollback, *Geochem. Geophys. Geosyst.*, *7*, Q03012, doi:10.1029/2005GC001056.

Stiros, S. C., and A. Drakos (2000), Geodetic constraints on the fault pattern of the 1978 Thessaloniki (northern Greece) earthquake (M-s = 6.4), *Geophys. J. Int.*, *143*(3), 679–688, doi:10.1046/j.1365-246X.2000.00249.x.

Suckale, J., S. Rondenay, M. Sachpazi, M. Charalampakis, A. Hosa, and L. H. Royden (2009), High-resolution seismic imaging of the western Hellenic subduction zone using teleseismic scattered waves, *Geophys. J. Int.*, *178*(2), 775–791, doi:10.1111/j.1365-246X.2009.04170.x.

Suleiman, A. S., and D. I. Doser (1995), The seismicity, seismotectonics and earthquake hazards of Libya, with detailed analysis of the 1935 April 19, M = 7.1 earthquake sequence, *Geophys. J. Int.*, *120*(2), 312–322, doi:10.1111/j.1365-246X.1995.tb01820.x.

Taymaz, T., J. Jackson, and D. Mckenzie (1991), Active tectonics of the north and central Aegean Sea, *Geophys. J. Int.*, *106*(2), 433–490, doi:10.1111/j.1365-246X.1991.tb03906.x.

Torelli, L., M. Grasso, G. Mazzoldi, D. Peis, and D. Gori (1995), Cretaceous to Neogene structural evolution of the Lampedusa Shelf (Pelagian Sea, central Mediterranean), *Terra Nova*, *7*(2), 200–212, doi:10.1111/j.1365-3121.1995.tb00689.x.

van Hinsbergen, D. J. J., D. G. van der Meer, W. J. Zachariasse, and J. E. Meulenkamp (2006), Deformation of western Greece during Neogene clockwise rotation and collision with Apulia, *Int. J. Earth Sci.*, *95*(3), 463–490, doi:10.1007/s00531-005-0047-5.

Westaway, R. (1990), The Tripoli, Libya, earthquake of September 4, 1974: Implications for the active tectonics of the central Mediterranean, *Tectonics*, *9*(2), 231–248, doi:10.1029/TC009i002p00231.

Wortel, M. J. R., and W. Spakman (2000), Subduction and slab detachment in the Mediterranean-Carpathian region, *Science*, *290*(5498), 1910–1917, doi:10.1126/science.290.5498.1910.

Wüstefeld, A., G. Bokelmann, G. Barruol, and J. P. Montagner (2009), Identifying global seismic anisotropy patterns by correlating shear-wave splitting and surface-wave data, *Phys. Earth Planet. Inter.*, *176*(3–4), 198–212, doi:10.1016/j.pepi.2009.05.006.

Yilmaz, Y., S. C. Genç, O. F. Gürer, M. Bozcu, K. Yilmaz, Z. Karacik, S. Altunkaynak, and A. Elmas (2000), When did the western Anatolian grabens begin to develop?, in *Tectonics and Magmatism in Turkey and the Surrounding Area*, edited by E. Bozkurt, J. A. Winchester, and J. D. A. Piper, *Geol. Soc. Spec.Publ.*, 173, 353–384, doi:10.1144/GSL.SP.2000.173.01.17.

Zandt, G., and E. Humphreys (2008), Toroidal mantle flow through the western US slab window, *Geology*, *36*(4), 295–298, doi:10.1130/G24611A.1.